

Supporting Information

Bypassing Glutamic Acid Decarboxylase 1 (Gad1) Induced Craniofacial Defects with a Photoactivatable Translation Blocker Morpholino

Matthew J. O'Connor,[†] Lindsey L. Beebe,[‡] Davide Deodato,[†] Rebecca E. Ball,[§]
A. Tyler Page,[§] Ariel J. VanLeuven,[§] Kyle T. Harris,[¶] Sungdae Park,[‡] Vani Hariharan,[§]
James D. Lauderdale,^{§,#,*} and Timothy M. Dore,^{†,¶,*}

[†] *New York University Abu Dhabi, PO Box 129188, Abu Dhabi, United Arab Emirates*

[‡] *Department of Genetics, University of Georgia, Athens, Georgia, 30602, USA*

[§] *Department of Cellular Biology, University of Georgia, Athens, Georgia, 30602, USA*

[#] *Neuroscience Division of the Biomedical and Health Sciences Institute, Athens, Georgia, 30602, USA*

[¶] *Department of Chemistry, University of Georgia, Athens, Georgia, 30602 USA*

*Corresponding Authors: E-mail: timothy.dore@nyu.edu, jdlauder@uga.edu

Table of Contents

Preparation of ccMOs.....	3
Scheme S1. Synthesis of 21.	7
NMR Spectra and Selected HPLC Chromatograms	9
¹ H NMR spectrum of compound 6.	9
¹ H NMR spectrum of compound 7.	10
HPLC chromatogram of compound 7.	10
¹ H NMR spectrum of compound 1a.	11
¹ H NMR spectrum of compound 8.	12
¹³ C NMR spectrum of compound 8.	12
¹ H NMR spectrum of compound 9.	13
¹³ C NMR spectrum of compound 9.	13
¹ H NMR spectrum of compound 10.	14
¹³ C NMR spectrum of compound 10.	14
¹ H NMR spectrum of compound 13.	15
HPLC chromatogram of compound 13.	15
¹ H NMR spectrum of compound 14.	16
HPLC chromatogram of compound 14.	16
¹ H NMR spectrum of compound 1b.	17
HPLC chromatogram of compound 1b.	17
¹ H NMR spectrum of compound 16.	18
¹³ C NMR spectrum of compound 16.	18
¹ H NMR spectrum of compound 17.	19
¹³ C NMR spectrum of compound 17.	19
¹ H NMR spectrum of compound 18.	20
¹³ C NMR spectrum of compound 18.	20
¹ H NMR spectrum of compound 19.	21
¹ H NMR spectrum of compound 21.	22
¹³ C NMR spectrum of compound 21.	22
UV-vis Spectra	23

Figure S1. UV-vis spectrum of CyHQ- <i>gad1b</i> -cMO (4b-1) in water.....	23
Figure S2. UV-vis spectrum of CyHQ- <i>gad2</i> -cMO (4b-2) in water.....	23
Photochemistry.....	24
Figure S3. Superimposition of the HPLC traces of CyHQ- <i>gad1b</i> -cMO (4b-1) before (red line) and after photolysis (black line).	24
Figure S4. Deconvoluted MS trace of CyHQ- <i>gad1b</i> -cMO (4b-1) prior to photolysis.	24
Figure S5. Deconvoluted MS trace of CyHQ- <i>gad1b</i> -cMO (4b-1) after photolysis.	24
Stability Toward Enzymatic Degradation.....	25
Figure S6. Enzymatic Stability of CyHQ- <i>gad2</i> -cMO (4b-2).....	25
Figure S7. Enzymatic Stability of <i>gad2</i> -MO (2-2).....	26
Figure S8. Enzymatic Stability of CyHQ-linker-PEG (21).	27
Zebrafish Studies	28
Figure S9. MO knockdown of <i>gad1b</i> , but not <i>gad2</i> causes morphological defects in craniofacial development.	28
Figure S10. MO knockdown of <i>gad1b</i> correlates with smaller, abnormally developed cranial cartilages in flat-mounted samples.....	29
Figure S11. Knockdown of <i>gad1b</i> causes aberrant chondrocyte morphology and stacking that can be rescued by co-injection with synthetic <i>gad1b</i> mRNA.	30
Figure S12. Knockdown of <i>gad1b</i> , but not <i>gad2</i> leads to smaller cranial cartilages.....	31
Figure S13. Expression of Gad1 and Gad2 proteins in developing zebrafish.	32
Figure S14. Sequence of <i>gad1b</i> exons 2 through 4.	33
Figure S15. Titration of <i>gad1b</i> translation blocking morpholino.....	34
Figure S16. The <i>gad1b</i> MO knockdown at 0.3 ng per embryo is effective through 3 dpf.	35
Figure S17. Titration of <i>gad2</i> translation blocking morpholino.....	36
Figure S18. The <i>gad2</i> MO knockdown at 1 ng per embryo is effective through 5 dpf.	37
Figure S19. Western blot analysis of BHQ- <i>gad1b</i> -ccMO and CyHQ- <i>gad1b</i> -ccMO.	38
Figure S20. Western blot analysis of <i>gad1b</i> splice blocking morpholino.	39
Figure S21. Knockdown of <i>gad1b</i> using a splice blocking MO causes morphological defects in the zebrafish head skeleton.	40
Figure S22. The <i>gad1b</i> translation blocking morphants exhibit altered expression of early neural crest markers <i>foxd3</i> , <i>tfap2a</i> , and <i>snail1b</i>	41
Figure S23. The <i>gad1b</i> translation blocking morphants exhibit altered distribution of <i>foxd3</i> or <i>sox10</i> expressing cells and an increase in acridine orange (AO) staining at 1 dpf.	42
Figure S24. Embryos harboring caged- <i>gad1b</i> translation blocking morpholinos exhibit normal expression of early neural crest markers <i>dlx2a</i> and <i>foxd3</i> at 10-12 somites of development.	43
Figure S25. Treatment with GABA _A modulators phenocopy <i>gad1b</i> knockdown and exhibit reduced expression of <i>dlx2a</i> and altered expression of <i>foxd3</i>	44
Figure S26. Knockdown of <i>gad1b</i> and <i>gad2</i> causes an increase in native neurological activity in 3 dpf zebrafish larvae.....	45
Figure S27. The <i>gad1b</i> synthetic mRNA is translated into Gad1b protein and can rescue morphant phenotype.	46
Preparation of Synthetic <i>gad1b</i> mRNA	47
Construction of the <i>gad1b</i> clone for preparing synthetic <i>gad1b</i> mRNA.....	47
In vitro transcription.	47
Microinjection.....	47

Preparation of ccMOs

General Synthetic Procedures. All reactions were carried out using glassware except for morpholino couplings, which were performed in microcentrifuge tubes. All other reagents and solvents were purchased from commercial sources and used without further purification unless specifically noted. ^1H and ^{13}C NMR were recorded on a Bruker Avance III HD 500 MHz or 600 MHz spectrometer. UV spectra for MO quantification were recorded on a Nanodrop 2000c. HPLC (analytical and preparative) was performed on an Agilent Infinity series system with an autosampler and diode array detector using Zorbax eclipse C-18 reverse phase columns. HRMS/LC-MS was performed on an Agilent 6540 HD Accurate Mass QTOF/LC/MS with electrospray ionization (ESI).

8-(8-Bromo-7-hydroxyquinolin-2-yl)-5,11-dimethyl-6,12-dioxo-7-oxa-2,5,11-triazaheptadecan-17-oic acid (6). Alcohol **5** (92 mg, 0.155 mmol), prepared using literature protocol,¹ was added to a solution of carbonyldiimidazole (628 mg, 3.87 mmol) in CH_2Cl_2 (25 mL). The reaction was monitored by TLC using a 1:1 acetone/chloroform solution. When TLC indicated the disappearance of starting material (~15 min), water (5 mL) was added and the organic layer separated, dried over anhydrous Na_2SO_3 , filtered, and evaporated in vacuo. The remaining residue was dissolved in CH_2Cl_2 and the resulting solution cooled in ice bath. *N,N'*-Dimethylethylenediamine (2 mL) was added rapidly and the reaction was monitored by TLC until completion (~15 min). Water (5 mL) was added and the organic layer separated and evaporated in vacuo. The resulting residue was dissolved in a solution of 1:1 acetonitrile/0.4 N NaOH (30 mL). The resulting solution was stirred in the dark until LC-MS indicated that the benzenesulfonyl group was removed and the ester was hydrolyzed (3-12 h). The reaction was neutralized to pH 8 followed by evaporation of the solvent in vacuo. The remaining residue was purified by HPLC (acetonitrile/water) to afford **6** as a yellow gum (30.3 mg, 0.054 mmol, 15%): ^1H NMR (600 MHz, CD_3OD) δ 8.30-8.19 (m, 1H), 7.82-7.73 (m, 1H), 7.52-7.37 (m, 1H), 7.35-7.25 (m, 1H), 6.06-5.70 (m, 1H), 3.81-3.49 (m, 3H), 3.26-3.11 (m, 4H), 3.09-3.05 (m, 1H), 3.04-2.99 (m, 2H), 2.98-2.93 (m, 1H), 2.87-2.82 (m, 1H), 2.81-2.77 (m, 1H), 2.76-2.67 (m, 1H), 2.62-2.58 (m, 1H), 2.51-2.18 (m, 6H), 1.74-1.49 (m, 5H), 1.50-1.23 (m, 2H); HRMS-ESI-LC-MS-Q-TOF (*m/z*) [$\text{M}+\text{H}$]⁺ calcd for $\text{C}_{24}\text{H}_{33}\text{BrN}_4\text{O}_6$ 553.1656 (^{79}Br) and 555.1636 (^{81}Br), found 553.1689 and 555.1674.

9-(8-Bromo-7-hydroxyquinolin-2-yl)-1-chloro-3,6,12-trimethyl-2,7,13-trioxo-8-oxa-3,6,12-triazaoctadecan-18-oic acid (7). Amine **6** (30.3 mg, 0.055 mmol) was stirred in dry acetonitrile (25 mL). DIEA (58 μL , 0.33 mmol) was added followed by chloroacetyl chloride (21.5 μL , 0.27 mmol). The resulting solution was stirred until LC-MS indicated the presence of the amide and phenolic ester (~15 min). The solvent was removed in vacuo and the resulting residue was dissolved in water (4 mL) and TFA (200 μL) and stirred until LC-MS indicated that the phenolic ester was hydrolyzed. The solvent was evaporated in vacuo and the resulting residue was purified by HPLC (acetonitrile/water) to provide **7** as a sticky gum (11.3 mg, 0.089 mmol, 33%): ^1H NMR (600 MHz, CD_3OD) δ 8.30-8.18 (m, 1H), 7.82-7.73 (m, 1H), 7.52-7.35 (m, 1H), 6.01-5.83 (m, 1H), 4.27-4.07 (m, 1H), 3.85-3.39 (m, 7H), 3.26-3.09 (m, 2H), 3.09-3.04 (m, 2H), 3.03-2.92 (m, 3H), 2.86-2.80 (m, 1H), 2.53-2.18 (m, 6H), 1.71-1.41 (m, 4H), 2.39-1.24 (m, 2H); HRMS-ESI-LC-MS-Q-TOF (*m/z*) [$\text{M}+\text{H}$]⁺ calcd for $\text{C}_{26}\text{H}_{34}\text{BrClN}_4\text{O}_7$ 629.1378 (^{79}Br , ^{35}Cl), 631.1357 (^{81}Br , ^{35}Cl), 630.1348 (^{79}Br , ^{37}Cl), and 632.1382 (^{81}Br , ^{37}Cl) found 629.1372 (^{79}Br , ^{35}Cl), 631.1358 (^{81}Br , ^{35}Cl), 630.1397 (^{81}Br , ^{37}Cl) and 632.1378 (^{79}Br , ^{37}Cl).

2,5-Dioxopyrrolidin-1-yl 9-(8-bromo-7-hydroxyquinolin-2-yl)-1-chloro-3,6,12-trimethyl-2,7,13-trioxo-8-oxa-3,6,12-triazaoctadecan-18-oate (1a). To a solution of **7** (5.2 mg, 0.0083 mmol) in dry acetonitrile/acetonitrile, pyridine (32 μ L, 0.406 mmol) and dissuccinimidyl carbonate (52 mg, 0.203 mmol) were added. Once HPLC or LC-MS indicated the reaction was complete (2-12 h) the solvent was removed in vacuo and the resulting residue was purified by HPLC (acetonitrile/water 0.1% TFA). Fractions containing only **1a** were combined, maintained at cold temperature to avoid reversion to **7**, and lyophilized to provide **1a** as a sticky solid (1.4 mg, 0.0019 mmol, 23%): $^1\text{H NMR}$ (600 MHz, CD_3OD) δ 8.31-8.18 (m, 1H), 7.82-7.74 (m, 1H), 7.51-7.37 (m, 1H), 7.32-7.24 (m, 1H), 6.01-5.82 (m, 1H), 4.39-3.40 (m, 6H), 3.26-3.01 (m, 6H), 3.01-2.91 (m, 3H), 2.87-2.79 (m, 4H), 2.87-2.79 (m, 4H), 2.73-2.13 (m, 5H), (m, 5H), 1.82-1.54 (m, 5H); HRMS-ESI-LC-MS-Q-TOF (m/z) $[\text{M}+\text{H}]^+$ calcd for $\text{C}_{30}\text{H}_{37}\text{BrClN}_5\text{O}_9$ 726.1541 (^{79}Br , ^{35}Cl), 728.1521 (^{81}Br , ^{35}Cl), 727.1575 (^{79}Br , ^{37}Cl), and 728.1512 (^{81}Br , ^{37}Cl) found 726.1540 (^{79}Br , ^{35}Cl), 728.1522 (^{81}Br , ^{35}Cl), 727.1578 (^{79}Br , ^{37}Cl) and 729.1553 (^{81}Br , ^{37}Cl).

7-((2-Methoxyethoxy)methoxy)-2-methylquinoline-8-carbonitrile (8). A mixture of 7-hydroxy-2-methylquinoline-8-carbonitrile (1.4 g, 7.4 mmol) prepared as previously described,² and diisopropylethylamine (1.09 mL, 9.7 mmol) were dissolved in anhydrous CH_2Cl_2 (35 mL). A solution of methoxyethoxymethyl chloride (1.1 mL 9.7 mmol) in CH_2Cl_2 (4 mL) was then added to the solution via addition funnel dropwise over 30 minutes. The reaction mixture was stirred for three hours at room temperature under nitrogen and monitored by TLC (hexanes/EtOAc 1:3). The solvent was removed *in vacuo*, and the residue was dissolved in EtOAc (150 mL) and washed twice with water (50 mL) and then dried over anhydrous Na_2SO_4 . Solvent was removed *in vacuo*, and the residue was purified by silica gel column chromatography (hexanes/EtOAc 1:1) to yield the product as a yellow oil (1.4 g, 8.2 mmol, 64%): $^1\text{H NMR}$ (600 MHz CDCl_3) δ 8.01 (d, $J = 8.3$ Hz, 1H), 7.92 (d, $J = 9.1$ Hz, 1H), 7.51 (d, $J = 8.3$ Hz, 1H), 7.28 (d, $J = 8.3$ Hz, 1H), 5.53 (s, 3H), 3.95 (t, 2H, $J = 4.4$ Hz) 3.58 (t, 2H, $J = 4.4$ Hz), 2.88 (s, 3H); $^{13}\text{C NMR}$ (600 MHz CDCl_3) δ 162.4, 161.8, 148.6, 156.0, 133.5, 121.8, 121.7, 114.7, 99.4, 94.0, 71.4, 68.6, 59.0, 25.7; HRMS-ESI-LC-MS-Q-TOF (m/z) $[\text{M}+\text{H}]^+$ calcd for $\text{C}_{15}\text{H}_{16}\text{N}_2\text{O}_3$ 273.1234, found 273.1231.

2-Formyl-7-((2-methoxyethoxy)methoxy)quinoline-8-carbonitrile (9). A mixture of SeO_2 (1.2 g, 11 mmol) and 1,4-dioxane (40 mL) and *tert*-butyl-hydroperoxide (70%, 727 mg, 5.28 mmol) was heated to 45 $^\circ\text{C}$ and stirred for 1 h. Quinoline **8** (1.0 g, 5.3 mmol) in 1,4-dioxane (10 mL) was added. After stirring at 45 $^\circ\text{C}$ for 3 h, the reaction was cooled and vacuum filtered. The filtrate was collected and concentrated, leaving a yellow solid. Purification was performed by silica gel column chromatography (hexanes/ethyl acetate 1:3) gave **9** as a yellow oil (1 g, 8.1 mmol, 74%): $^1\text{H NMR}$ (600 MHz, CDCl_3) δ 10.3 (s, 1H), 8.33 (d, $J = 8.3$ Hz, 1H), 8.09 (d, $J = 9.2$ Hz, 1H), 8.00 (d, $J = 8.3$ Hz, 1H), 7.76 (d, $J = 9.2$ Hz, 1H), 5.59 (s, 3H), 4.15 (t, $J = 4.0$ Hz, 2H) 3.59 (t, $J = 4.0$ Hz, 2H); $^{13}\text{C NMR}$ (120 MHz, CDCl_3) δ 193.4, 162.8, 153.9, 148.3, 137.8, 133.8, 125.2, 118.4, 117.0, 114.0, 100.2, 94.2, 71.3, 68.2, 59.0; HRMS-ESI-LC-MS-Q-TOF (m/z) $[\text{M}+\text{H}]^+$ calcd for $\text{C}_{15}\text{H}_{14}\text{N}_2\text{O}_4$ 287.1026, found 273.1038.

2-(1-hydroxybut-3-en-1-yl)-7-((2-methoxyethoxy)methoxy)quinoline-8-carbonitrile (10). A suspension of **9** (414 mg, 1.45 mmol), allyl bromide (1.0 mL, 7.3 mmol), indium powder (170 mg, 1.5 mmol), THF (5 mL), and sat. NH_4Cl (5 mL) solution was sonicated at 55 $^\circ\text{C}$ for 3 h. The crude reaction mixture was filtered through a celite plug then extracted into EtOAc (100 mL), washed with water (20 mL), and dried with Na_2SO_4 . The solvent and excess allyl bromide were then removed in vacuo to afford **10** (450 mg, 6.9 mmol, 95%): $^1\text{H NMR}$ (600 MHz, CDCl_3) δ 8.16 (d, $J = 8.4$ Hz, 1H), 8.01 (d, $J = 9.1$ Hz, 1H) 7.61 (d, $J = 9.1$ Hz, 1H), 7.42 (d, $J = 8.4$ Hz, 1H),

5.88 (m, 1H), 5.57 (s, 2H), 5.17-5.07 (m, 2H), 5.05-4.99 (m, 1H), 3.98 (t, $J = 4.4$ Hz, 2H), 3.60 (t, $J = 4.4$ Hz, 2H), 2.81-2.70 (m, 1H), 2.62-2.51 (m, 1H); ^{13}C NMR (600 MHz, CDCl_3) δ 164.5, 162.2, 147.1, 136.9, 133.6, 122.7, 118.4, 118.2, 115.6, 114.4, 99.4, 94.1, 72.4, 71.4, 68.7, 59.0, 42.5; HRMS-ESI-LC-MS-Q-TOF (m/z) $[\text{M}+\text{H}]^+$ calcd for $\text{C}_{18}\text{H}_{20}\text{N}_2\text{O}_4$ 329.1496 found 329.1503.

2-(1-Hydroxy-3-oxopropyl)-7-((2-methoxyethoxy)methoxy)quinoline-8-carbonitrile (11). To a solution of **10** (550 mg, 1.6 mmol) in THF/water (1:1, 8 mL) were added 2,6-lutidine (0.49 mL, 4.1 mmol) and $\text{K}_2\text{OsO}_4 \cdot 2\text{H}_2\text{O}$ (6 mg, 0.016 mmol). After 15 min, NaIO_4 (1.40 g, 4.1 mmol) was added. The reaction was stirred at 25 °C overnight. The reaction mixture was then filtered through a celite plug with CH_2Cl_2 (40 mL). The organic layer was separated, and the aqueous layer was extracted with CH_2Cl_2 (3 \times 10 mL). The combined organic phases were washed with brine (5 \times 10 mL) to remove hydrophilic impurities and then dried over Na_2SO_4 . The solvent was removed, and the product was flushed through a silica gel chromatography column to afford **11** (550 mg) as an impure yellow oil: HRMS-ESI-LC-MS-Q-TOF (m/z) $[\text{M}+\text{H}]^+$ calcd for $\text{C}_{17}\text{H}_{18}\text{N}_2\text{O}_4$ 331.1288, found 331.1297. The material was taken immediately to the next step without further purification as it quickly discolors and degrades.

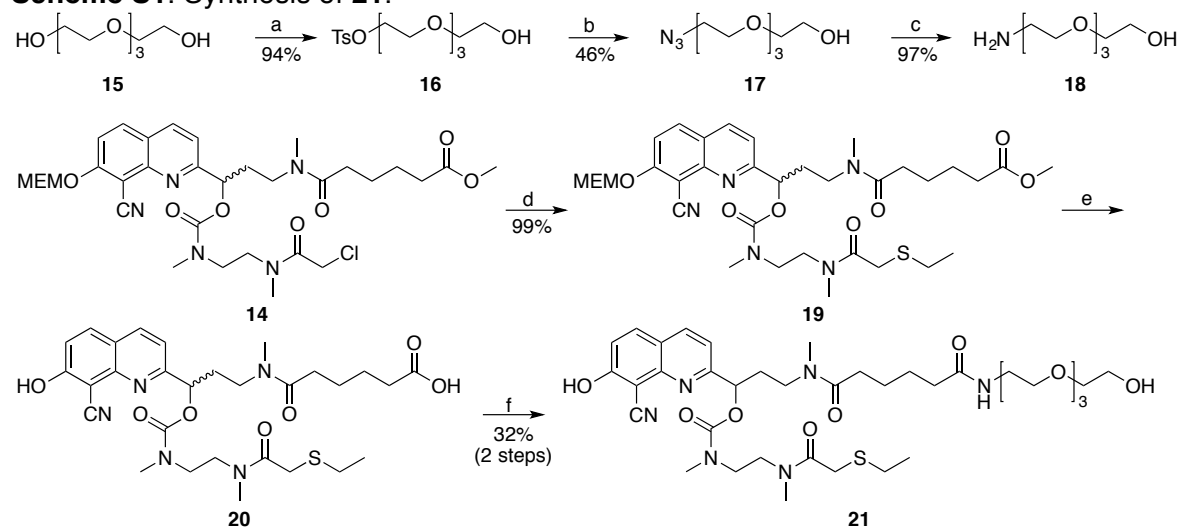
2-(1-Hydroxy-3-(methylamino)propyl)-7-((2-methoxyethoxy)methoxy)quinoline-8-carbonitrile (12). To a solution of **11** (1.2 g, 3.5 mmol) in THF (100 mL) was added 2.0 M methylamine solution in MeOH (2.6 mL, 5. mmol) and two drops of acetic acid. After 30 min, sodium acetoxy borohydride (970 mg, 4.6 mmol) was added and stirred at rt until LC-MS indicated that it was complete (3-12 h). The reaction was quenched with 0.4 N NaOH, extracted in CH_2Cl_2 , and evaporated to a crude mixture containing **12** (1.3 g) that was immediately taken on to the next step: HRMS-ESI-LC-MS-Q-TOF (m/z) $[\text{M}+\text{H}]^+$ calcd for $\text{C}_{18}\text{H}_{23}\text{N}_3\text{O}_4$ 346.1761, found 346.1761.

Methyl 6-((3-(8-cyano-7-((2-methoxyethoxy)methoxy)quinolin-2-yl)-3-hydroxypropyl)(methyl)amino)-6-oxohexanoate (13). Under a nitrogen atmosphere, amine **12** (1.3 g, 0.33 mmol) and *N,N*-diisopropylethylamine (65 μL , 0.37 mmol) were dissolved in anhydrous CH_2Cl_2 (5 mL), and the resulting solution cooled to 0 °C. Methyl adipoyl chloride (230 μL , 0.173 mmol) was added over 5 min, and the reaction mixture was stirred for 6 h at rt under nitrogen. The solvent was removed in vacuo, and the resulting residue was dissolved in CH_2Cl_2 (40 mL). The resulting solution was washed twice with saturated, aqueous NaHCO_3 and then dried over anhydrous Na_2SO_4 . The solvent was removed in vacuo, and the residue was purified by silica gel column chromatography (chloroform/THF 1:1) to yield **13** (0.53 mg, 0.14 mmol, 38%) as a yellow oil: ^1H NMR (600 MHz, CDCl_3) δ 8.19-8.10 (m, 1H), 8.01-7.95 (m, 1H), 7.70-7.55 (m, 1H), 7.55 (s, 3H), 7.56-7.35 (m, 1H), 5.56-5.55 (m, 1H), 4.95-4.81 (m, 1H), 3.93 (t, 2H), 3.9-3.69 (m, 1H), 3.67-3.60 (m, 3H), 3.55 (t, 2H), 3.52-3.36 (m, 1H), 3.33 (s, 3H), 3.03-2.88 (m, 1H), 2.46-2.27 (m, 3H), 2.26-1.76 (m, 3H), 1.68-1.46 (m, 4H); HRMS-ESI-LC-MS-Q-TOF (m/z) $[\text{M}+\text{H}]^+$ calcd for $\text{C}_{25}\text{H}_{33}\text{N}_3\text{O}_7$ 488.2391, found 488.2397.

Methyl 1-chloro-9-(8-cyano-7-((2-methoxyethoxy)methoxy)quinolin-2-yl)-3,6,12-trimethyl-2,7,13-trioxo-8-oxa-3,6,12-triazaoctadecan-18-oate (14). A solution of **13** (250 mg, 0.553 mmol) in CH_2Cl_2 (4 mL) was added to a solution of carbonyl diimidazole (2.0 g, 12.3 mmol) in CH_2Cl_2 and the resulting solution was stirred until LC-MS indicated that the reaction was complete (~10 min). Water was added and the mixture was partitioned and the aqueous phase removed. Additional CH_2Cl_2 (20 mL) was added and the resulting solution was cooled to 0 °C. *N,N*-Dimethylethylene diamine (2.5 mL) was added and the resulting solution was stirred until LC-MS indicated that the reaction was complete (~10 min). The solvent was removed in vacuo and

the resulting residue was dissolved in CH₂Cl₂. The organic layer was washed with H₂O (5 mL) and dried with sodium sulfate, and the solvent removed in vacuo (it is critical at this stage to avoid exposing the free amine to acidic workups to prevent reversion of the carbamate to starting material). The resulting residue was dissolved in a solution of diisopropylethylamine (251 μL, 1.02 mmol) in CH₂Cl₂ (5 mL) and the resulting solution cooled to 0 °C. Chloroacetyl chloride (81 μL, 1.02 mmol) was added and the reaction was stirred for 4 h. Water was added, and the resulting mixture was extracted into CH₂Cl₂. The solvent was removed in vacuo and the resulting material was purified using column chromatography starting with a gradient of chloroform and THF (0 -100% THF over 20 minutes). Re-dissolving the material in CH₂Cl₂ and washing with water (3 times) removed the remaining impurities. The CH₂Cl₂ was removed in vacuo to provide carbamate **14** as a yellow oil (93 mg, 0.14 mmol, 25%). An additional 170 mg (0.24 mmol, 44%) of **14** was eluted from the column by applying another gradient to the column (0-100% methanol in CH₂Cl₂ over 10 minutes): ¹H NMR (600 MHz, CDCl₃) δ 8.20-8.10 (m, 1H), 8.01-7.93 (m, 1H), 7.62-7.53 (m, 1H), 7.50-7.35 (m, 1H), 5.95-5.82 (m, 1H), 5.50-5.50 (m, 2H), 4.35-3.74 (m, 5H), 3.73-3.40 (m, 10H), 3.34 (s, 2H), 3.23-2.77 (m, 8H), 2.64-2.15 (m, 6H), 2.05-1.90 (m, 1H), 1.85-1.75 (m, 1H), 1.65-1.50 (m, 4H); HRMS-ESI-LC-MS-Q-TOF (m/z) [M+H]⁺ calcd for C₃₂H₄₄CIN₅O₉ 678.2900, found 678.2889.

2,5-Dioxopyrrolidin-1-yl 1-chloro-9-(8-cyano-7-hydroxyquinolin-2-yl)-3,6,12-trimethyl-2,7,13-trioxo-8-oxa-3,6,12-triazaoctadecan-18-oate (1b). A solution of **14** (36 mg, 0.074 mmol) was prepared by dissolving **14** into 1:1 acetonitrile/water (20 mL) with 5% TFA. The mixture was stirred at 40 °C in the dark for 12 hours. The reaction was monitored by HPLC or LC-MS for the hydrolysis of both protecting group and methyl ester. The solvent was removed in vacuo to dryness forming an orange gum. The material was then dissolved in dry acetonitrile and then added pyridine (12 μL, 0.148 mmol) and dissuccinimidyl carbonate (38 mg, 0.148 mmol). The reaction was monitored by HPLC or LC-MS (2 h-overnight). Upon completion, the solvent was removed in vacuo and the residue was purified by silica gel column chromatography (methanol/CH₂Cl₂ 1:9) to yield **1b** (29 mg, 0.043 mmol, 58%) as a sticky solid. ¹H NMR (600 MHz, CD₃OD) δ 8.34-8.24 (m, 1H), 8.07-7.99 (m, 1H), 7.56-7.40 (m, 1H), 7.32-7.24 (m, 1H), 5.96-5.79 (m, 1H), 4.37-4.08 (m, 2H), 3.78-3.56 (m, 7H), 3.46-3.43 (m, 1H), 3.26-3.16 (m, 2H), 3.13-3.05 (m, 3H), 3.00-2.90 (m, 3H), 2.88-2.80 (m, 3H), 2.72-2.53 (m, 2H), 2.47-2.22 (m, 5H), 1.91-1.50 (m, 6H), 1.39-1.28 (m, 2H); HRMS-ESI-LC-MS-Q-TOF (m/z) [M+H]⁺ calcd for C₃₁H₃₇CIN₆O₉ 673.2383, found 673.2396.

Scheme S1. Synthesis of 21.

Reagents and conditions. (a) *para*-toluenesulfonyl chloride, NaOH, THF, 0 °C, 3 h; (b) sodium azide, EtOH, 70 °C, 12 h; (c) 10% Pd/C, H₂, MeOH, 3 h; (d) ethanethiol, NaOH, EtOH, 0 °C to rt, 1 h; (e) TFA, H₂O/CH₃CN, 40 °C, 12 h; (f) **18**, EDC, TBTU, DIEA, DMF, 0 °C to rt, 12 h.

2-(2-(2-(2-Hydroxyethoxy)ethoxy)ethoxy)ethyl 4-methylbenzenesulfonate (16). To a cold solution (0 °C) of tetraethylene glycol **15** (10.18 g, 52.4 mmol) in THF (3 mL), NaOH (356 mg, 8.9 mmol) was added. A solution of *para*-toluenesulfonyl chloride (1.0 g, 5.2 mmol) in THF (10 mL) was added dropwise with a dropping funnel and the resulting mixture was stirred at 0 °C for 3 h. The reaction mixture was quenched with water (50 mL), extracted with CH₂Cl₂ (3 x 50 mL) and the organic phase washed with water (2 x 50 mL). After drying over MgSO₄, the solvent was evaporated, affording **16** as an oil (1.7 g, 4.9 mmol, 94%): ¹H NMR (500 MHz, CDCl₃) δ 7.83-7.77 (d, *J* = 8.3, 1.8 Hz, 2H), 7.35 (d, *J* = 8.3, 1.8 Hz, 2H), 4.21-4.12 (t, *J* = 11.0, 3.6 Hz, 2H), 3.75-3.68 (m, 4H), 3.65 (dt, *J* = 8.6, 2.9 Hz, 4H), 3.60 (d, *J* = 1.9 Hz, 6H), 2.45 (s, 3H); ¹³C NMR (126 MHz, CDCl₃) δ 144.85, 132.92, 129.84, 127.97, 72.50, 70.72, 70.63, 70.44, 70.30, 69.26, 68.69, 61.70, 21.65.

2-(2-(2-(2-Azidoethoxy)ethoxy)ethoxy)ethan-1-ol (17). Sodium azide (1.6 g, 24.7 mmol) was added to a solution of **16** (1.7 g, 4.9 mmol) in EtOH (25 mL). The mixture was heated to 70 °C and stirred for 12h. After cooling water (25 mL) was added and the mixture concentrated to a third of his volume. The mixture was extracted with EtOAc (3 x 50 mL) and washed with water (2 x 50 mL). After drying over MgSO₄ solvent was evaporated affording **17** as an oil (0.5 g, 2.3 mmol, 46%): ¹H NMR (500 MHz, CDCl₃) δ 3.70 (t, *J* = 4.9, 2.5 Hz, 2H), 3.68-3.63 (m, 10H), 3.59 (t, *J* = 5.5, 2.1 Hz, 2H), 3.38 (t, *J* = 5.5, 2.1 Hz, 2H); ¹³C NMR (126 MHz, CDCl₃) δ 72.51, 70.67, 70.66, 70.62, 70.54, 70.29, 70.00, 61.66, 50.66, 50.64.

2-(2-(2-(2-Aminoethoxy)ethoxy)ethoxy)ethan-1-ol (18). A solution of **17** (0.2 g, 0.9 mmol) in MeOH (8 mL) was charged in a pressure vessel and stirred under hydrogen atmosphere (4 bars) for 3 h. The mixture was then diluted with MeOH (20 mL) and filtered over a celite pad. Solvent was evaporated furnishing primary amine **18** as an oil (170 mg, 0.9 mmol, 97%): ¹H NMR (500 MHz, CDCl₃) δ 3.73 (t, *J* = 5.0, 3.6 Hz, 2H), 3.67 (d, *J* = 7.4 Hz, 8H), 3.61 (dd, *J* = 5.0, 3.6 Hz, 2H), 3.56 (t, *J* = 5.0 Hz, 2H), 2.89 (t, *J* = 5.0 Hz, 2H), 2.72 (s, 2H). ¹³C NMR (126 MHz, CDCl₃) δ 73.00, 72.77, 70.58, 70.50, 70.20, 70.05, 61.47, 41.33; HRMS-ESI-LC-MS-Q-TOF (*m/z*) [M+H]⁺ calcd for C₈H₁₉NO₄ 194.1387, found 194.1381.

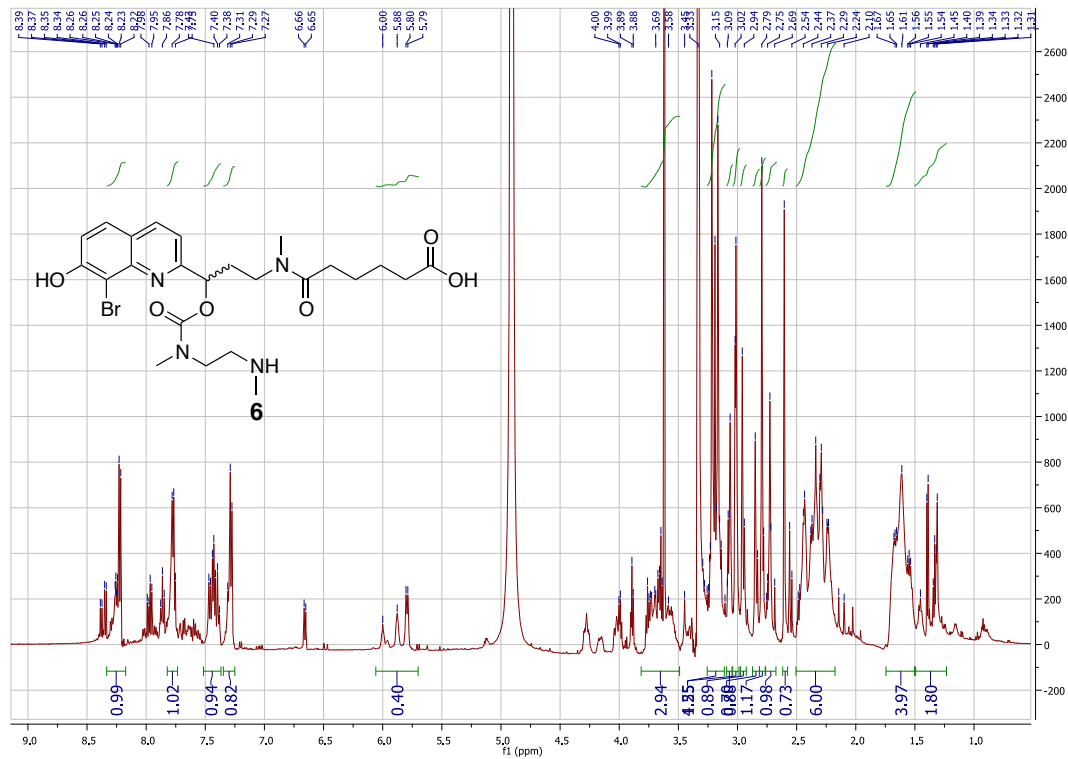
Methyl 12-(8-cyano-7-((2-methoxyethoxy)methoxy)quinolin-2-yl)-6,9,15-trimethyl-5,10,16-trioxo-11-oxa-3-thia-6,9,15-triazahenicosan-21-oate (19). To a cold solution of **14** (20 mg, 0.03 mmol) in EtOH (3 mL) a solution of ethanethiol (6 μ L, 0.08 mmol) and NaOH (3.3 mg, 0.08) in water (1 mL) was added dropwise. The temperature was raised to rt and the mixture was stirred for 1 h. The mixture was diluted with EtOAc (20 mL) and washed with water (2 x 20 mL). After drying over MgSO₄ solvent was evaporated affording **19** as a sticky solid (22 mg, 0.03 mmol, mixture of methyl and ethyl ester, 99%): ¹H NMR (500 MHz, CDCl₃) δ 8.24-8.08 (m, 1H), 7.97 (d, *J* = 9.5 Hz, 1H), 7.66-7.52 (m, 1H), 7.45 (dt, *J* = 20.9, 10.6 Hz, 1H), 5.90 (t, *J* = 6.2 Hz, 1H), 5.55 (s, 2H), 4.18-4.04 (m, 2H), 3.95 (t, *J* = 4.3 Hz, 2H), 3.81-3.40 (m, 10H), 3.37 (s, 3H), 3.30-3.10 (m, 4H), 3.06 (dd, *J* = 14.4, 4.0 Hz, 3H), 3.00-2.88 (m, 3H), 2.62 (t, *J* = 7.6 Hz, 2H), 2.46-2.14 (m, 6H), 1.71-1.53 (m, 3H), 1.25 (s, 3H); HRMS-ESI-LC-MS-Q-TOF (*m/z*) [M+H]⁺ calcd for C₃₄H₄₉N₅O₉S 704.3324, found 704.3329.

12-(8-Cyano-7-hydroxyquinolin-2-yl)-6,9,15-trimethyl-5,10,16-trioxo-11-oxa-3-thia-6,9,15-triazahenicosan-21-oic acid (20). To a solution of **19** (22 mg, 0.03 mmol) in a 1:1 mixture of CH₃CN/water (6 mL) trifluoroacetic acid (300 μ L) was added dropwise. The mixture was stirred at 40 °C in the dark for 12 h. After cooling the mixture was diluted with CH₃CN and evaporated. The dark oil obtained was used directly in the next step: HRMS-ESI-LC-MS-Q-TOF (*m/z*) [M+H]⁺ calcd for C₂₉H₃₉N₅O₇S 602.2643, found 602.2779.

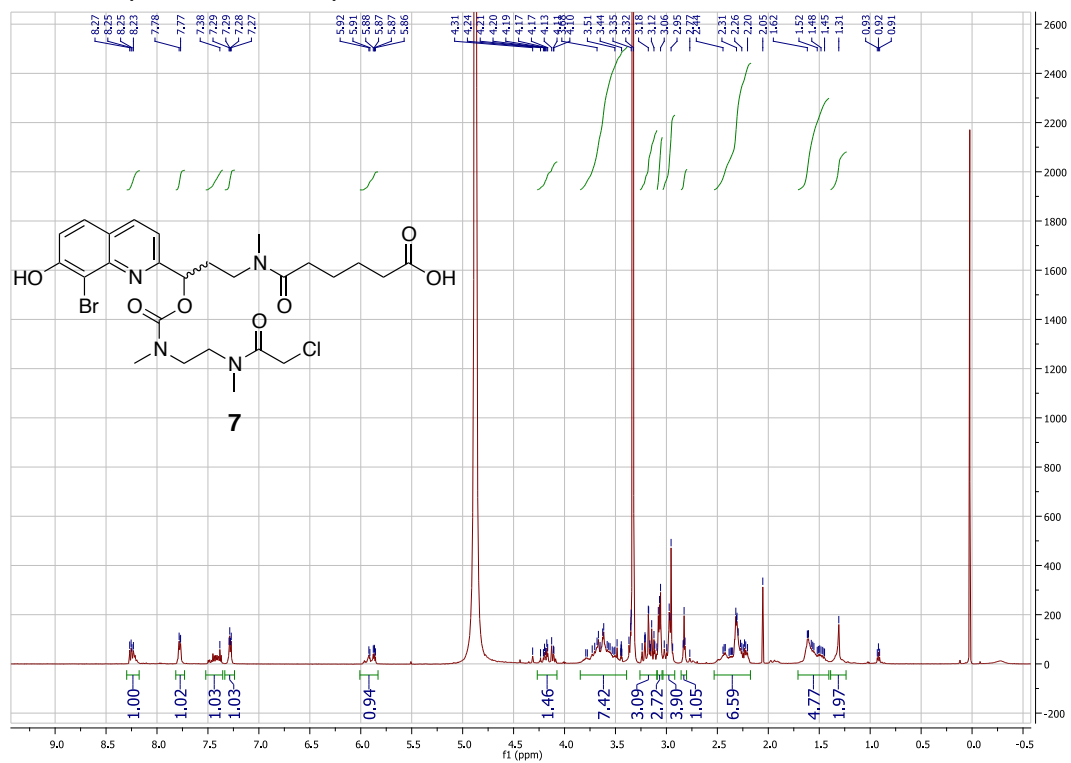
22-(8-Cyano-7-hydroxyquinolin-2-yl)-1-hydroxy-19-methyl-13,18-dioxo-3,6,9-trioxa-12,19-diazadocosan-22-yl (2-(2-(ethylthio)-N-methylacetamido)ethyl)(methyl)carbamate (21). To a cold solution of **20** (22 mg, 0.03 mmol) in DMF (1 mL), a solution of **18** (10 mg, 0.05 mmol) was added dropwise, followed by EDC (7 mg, 0.03 mmol), TBTU (11 mg, 0.03 mmol) and DIEA (6 μ L, 0.03 mmol). Temperature was raised to rt and the mixture was stirred in the dark for 12 h. MeOH (10 mL) was added and the mixture was evaporated. The residue was purified by silica gel chromatography (10% MeOH in CH₂Cl₂) followed by a second purification by prepHPLC (water/CH₃CN) affording pure compound **21** (9 mg, 0.01 mmol, 32%): ¹H NMR (500 MHz, CD₃OD) δ 8.35-8.25 (m, 1H), 8.04 (dd, *J* = 9.0, 6.1 Hz, 1H), 7.53-7.42 (m, 1H), 7.33-7.25 (m, 1H), 5.94-5.80 (m, 1H), 3.71-3.60 (m, 10H), 3.57 (dd, *J* = 5.5, 4.2 Hz, 3H), 3.54 (t, *J* = 5.2 Hz, 2H), 3.36 (t, *J* = 5.5 Hz, 2H), 3.33 (s, 10H), 3.18 (dd, *J* = 6.9, 4.6 Hz, 2H), 3.09 (dd, *J* = 6.6, 2.6 Hz, 2H), 3.00-2.92 (m, 3H), 2.61-2.53 (m, 1H), 2.41-2.27 (m, 3H), 2.27-2.14 (m, 2H), 1.67-1.50 (m, 4H), 1.27-1.14 (m, 3H); ¹³C NMR (126 MHz, CD₃OD) δ 174.60, 173.68, 170.88, 159.37, 137.47, 137.22, 137.12, 133.85, 117.84, 117.73, 94.54, 75.58, 72.25, 70.19, 70.15, 69.93, 69.81, 69.22, 69.20, 60.80, 48.10, 47.93, 47.76, 47.70, 47.59, 47.42, 47.25, 47.08, 46.09, 44.02, 38.95, 32.59, 32.50, 32.13, 29.37, 25.63, 25.25, 25.20, 24.26, 13.36; HRMS-ESI-LC-MS-Q-TOF (*m/z*) [M+H]⁺ calcd for C₃₇H₅₆N₆O₁₀S 777.3851, found 777.3852.

NMR Spectra and Selected HPLC Chromatograms

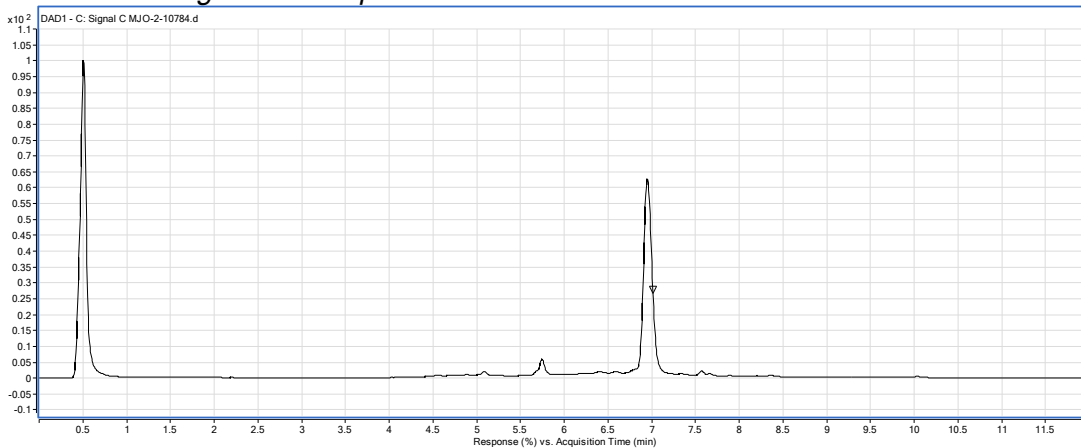
¹H NMR spectrum of compound 6.



¹H NMR spectrum of compound 7.

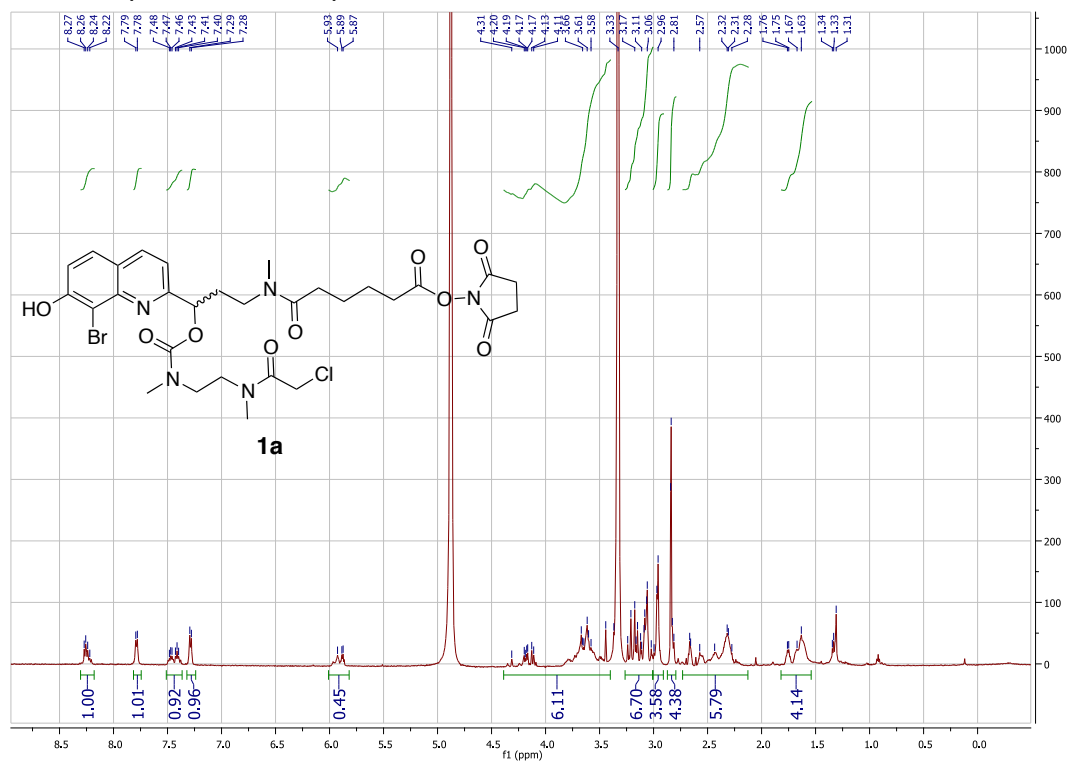


HPLC chromatogram of compound 7.

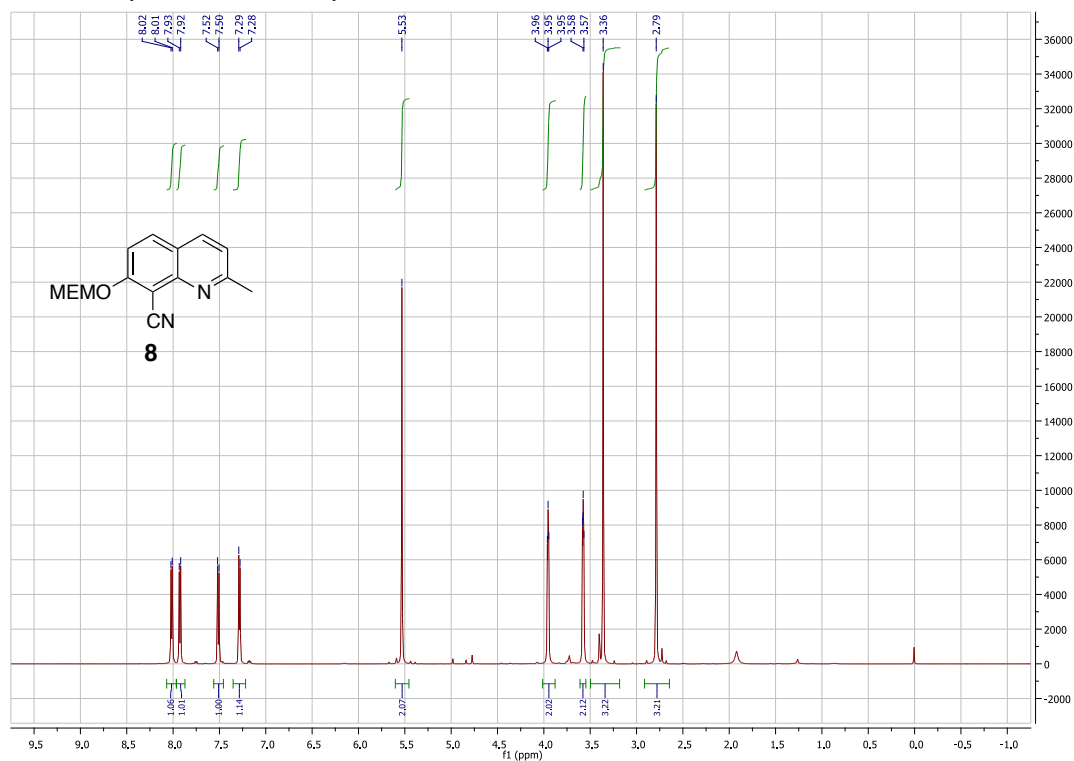


Method: 0-10 min, 5-100% acetonitrile/H₂O, 10-12 min 100% acetonitrile, monitor at 230 nm

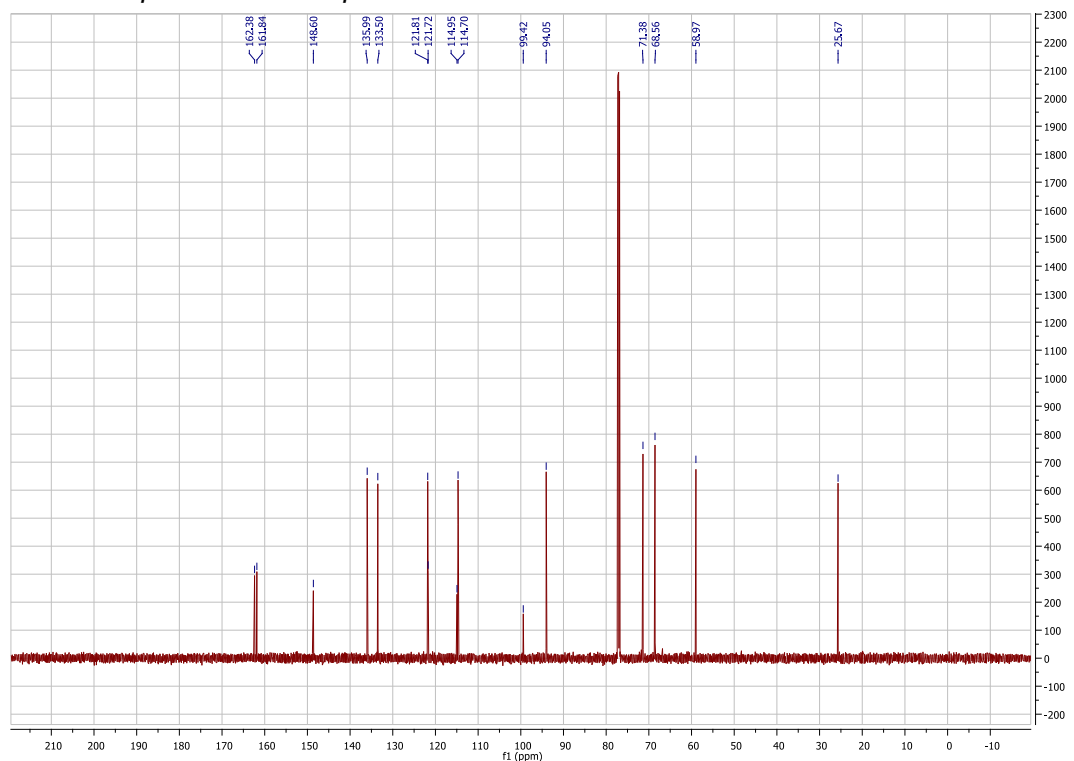
¹H NMR spectrum of compound **1a**.



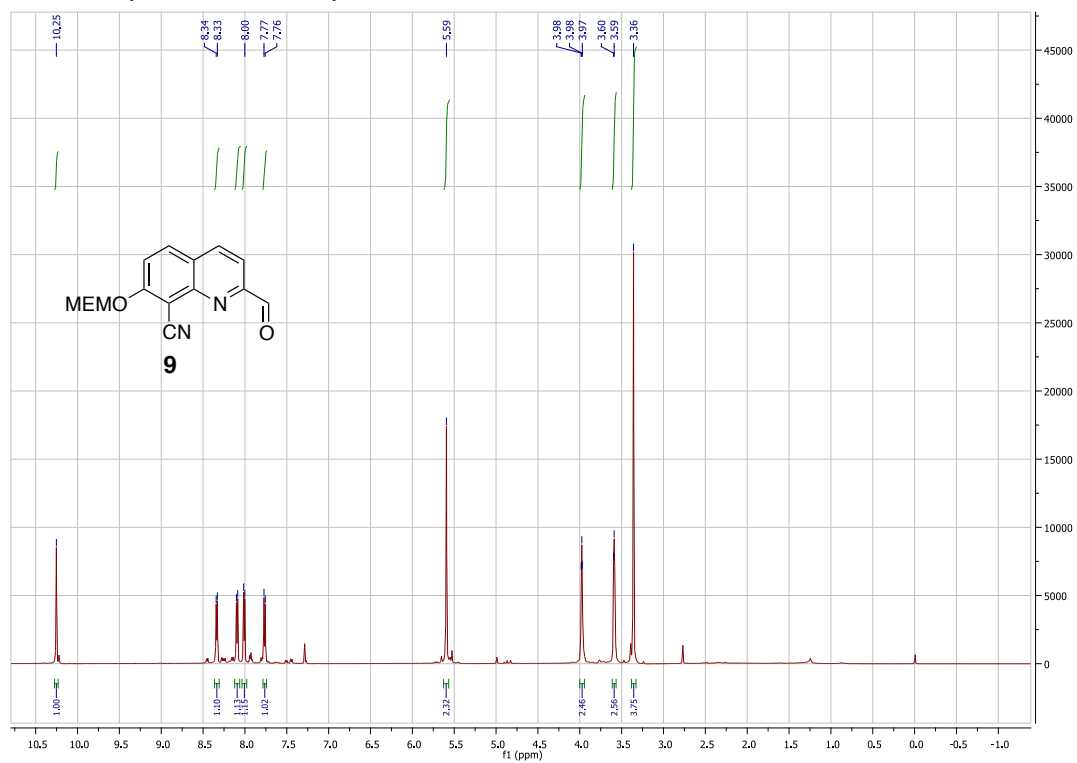
¹H NMR spectrum of compound **8**.



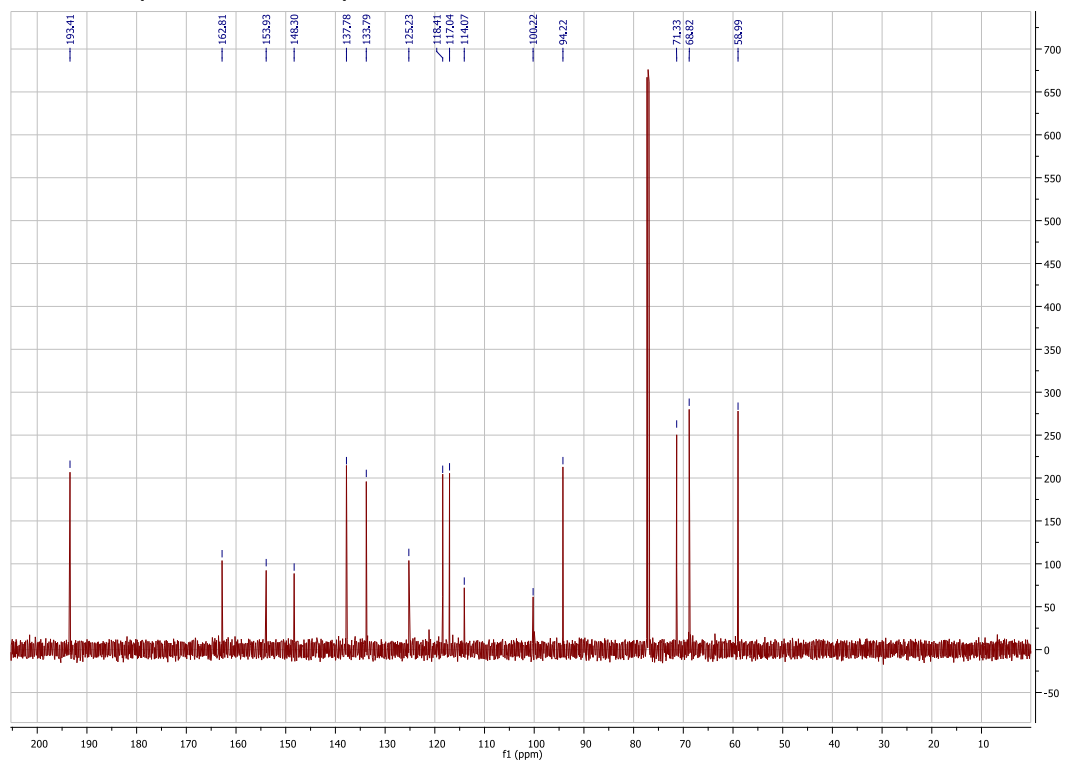
¹³C NMR spectrum of compound **8**.



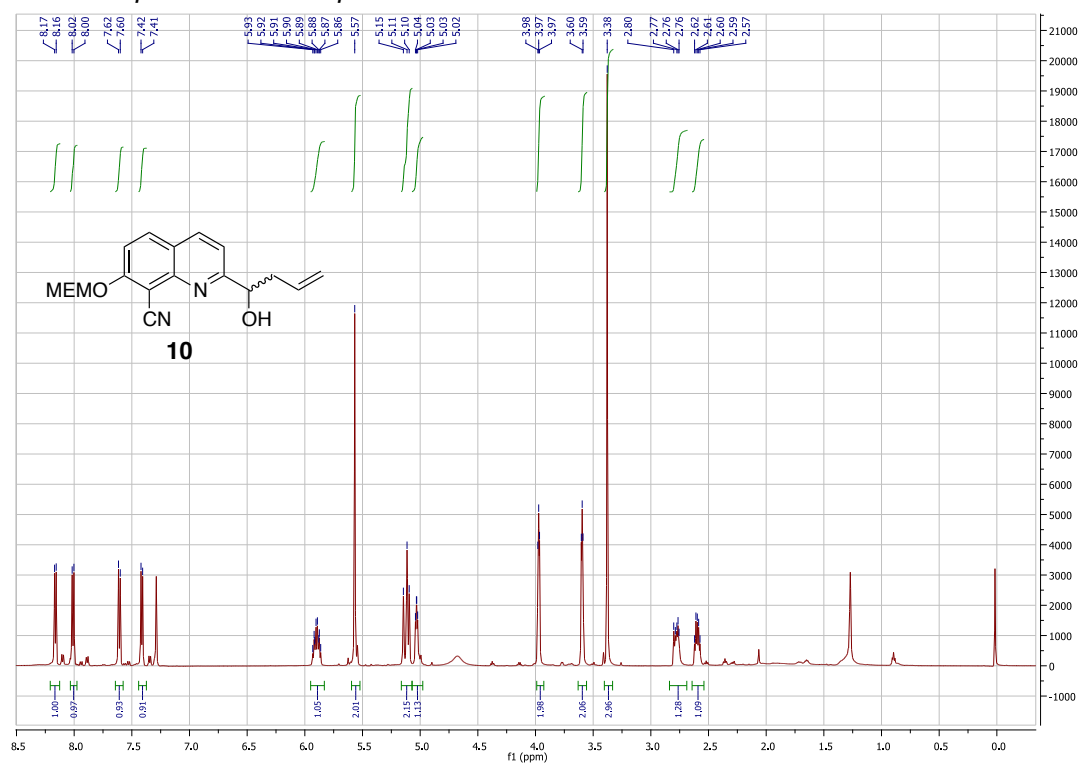
¹H NMR spectrum of compound **9**.



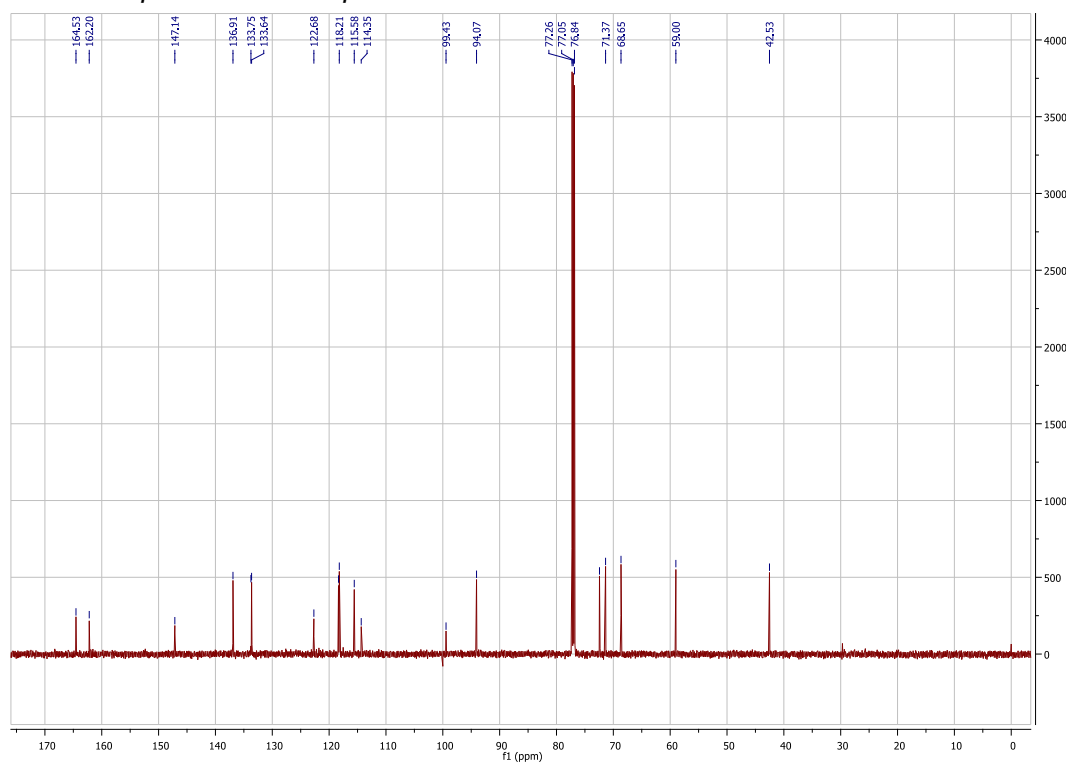
¹³C NMR spectrum of compound **9**.



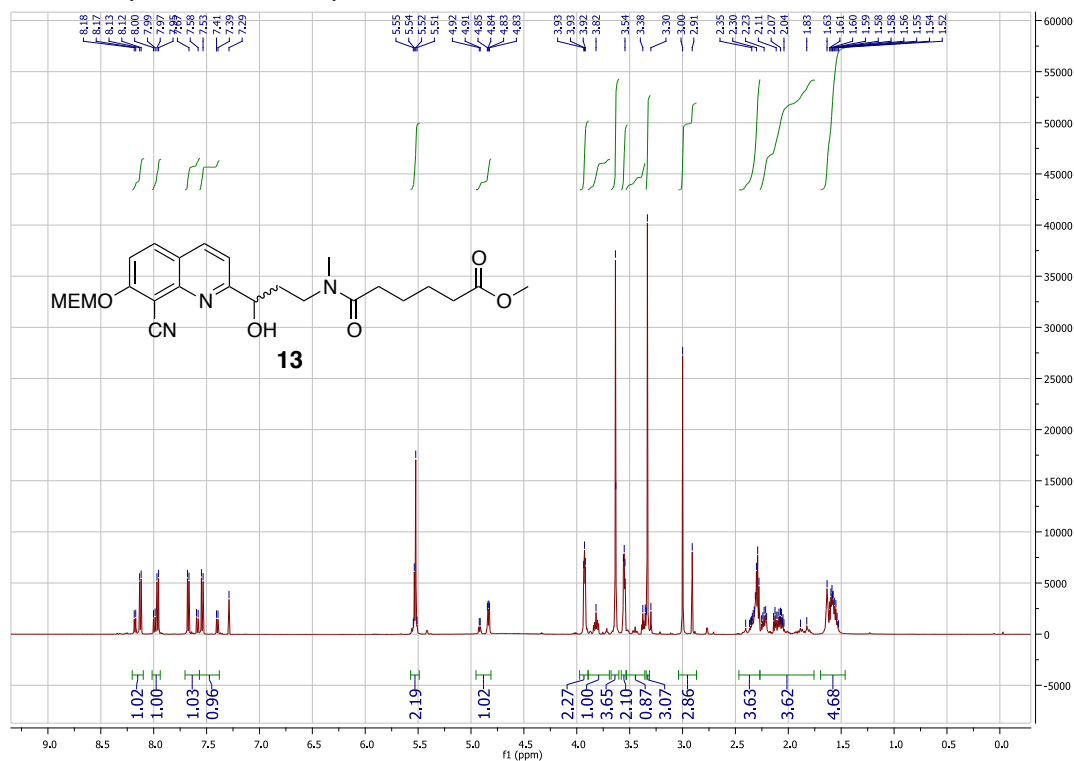
¹H NMR spectrum of compound 10.



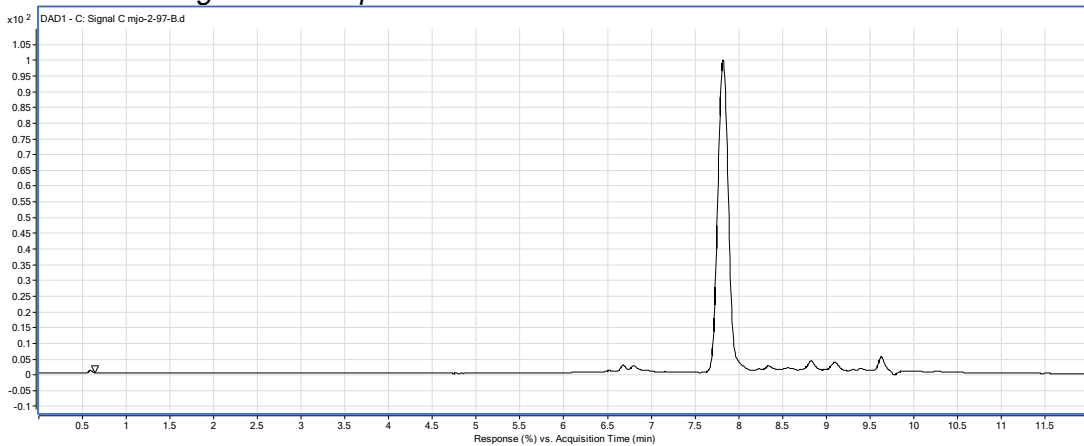
¹³C NMR spectrum of compound 10.



¹H NMR spectrum of compound **13**.

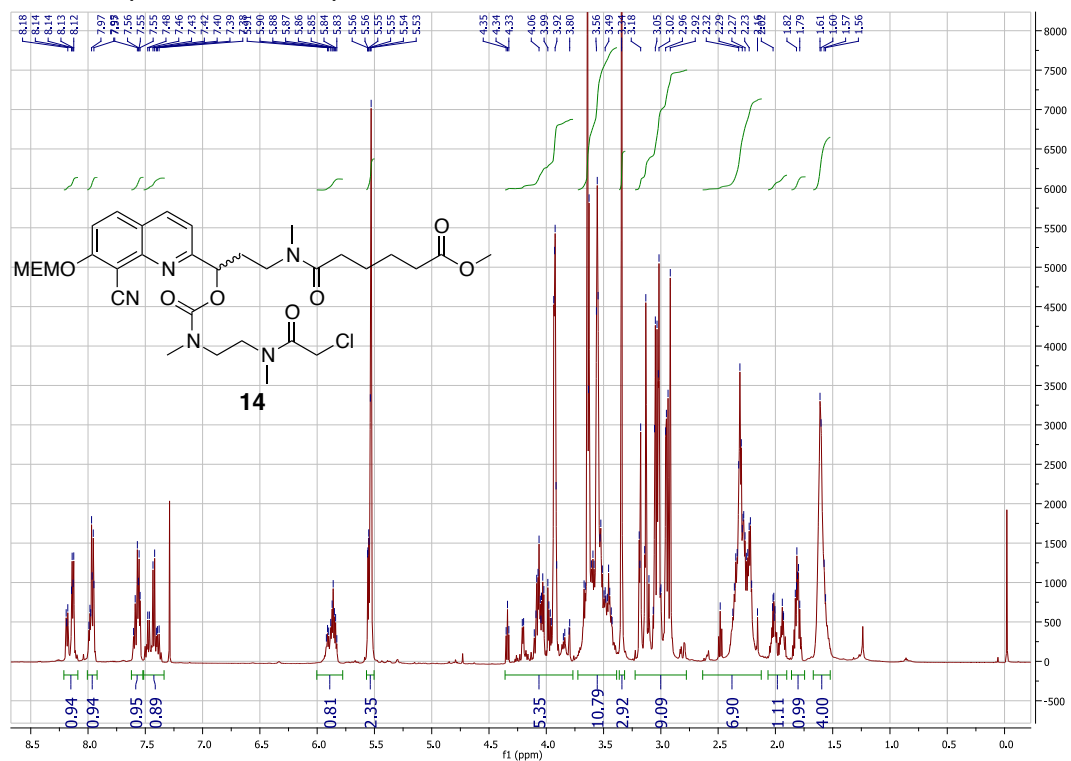


HPLC chromatogram of compound **13**.

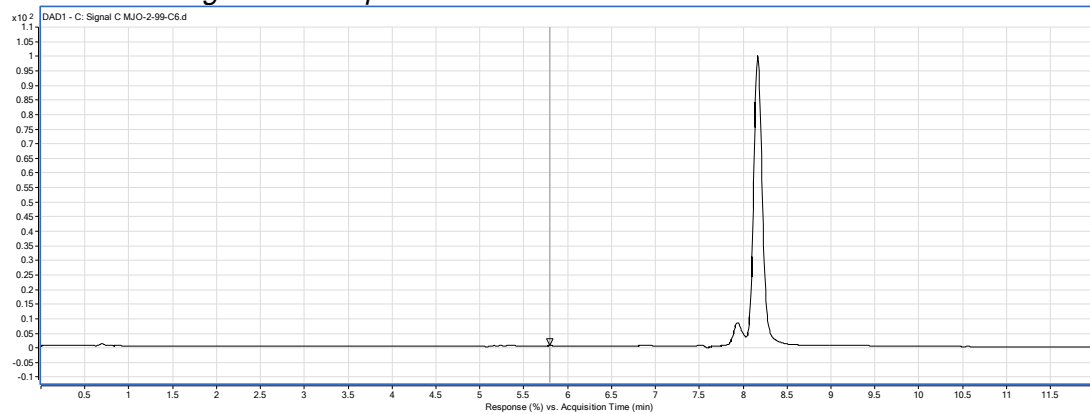


Method: 0-10 min, 5-100% acetonitrile/H₂O, 10-12 min 100% acetonitrile, monitor at 230 nm

¹H NMR spectrum of compound **14**.

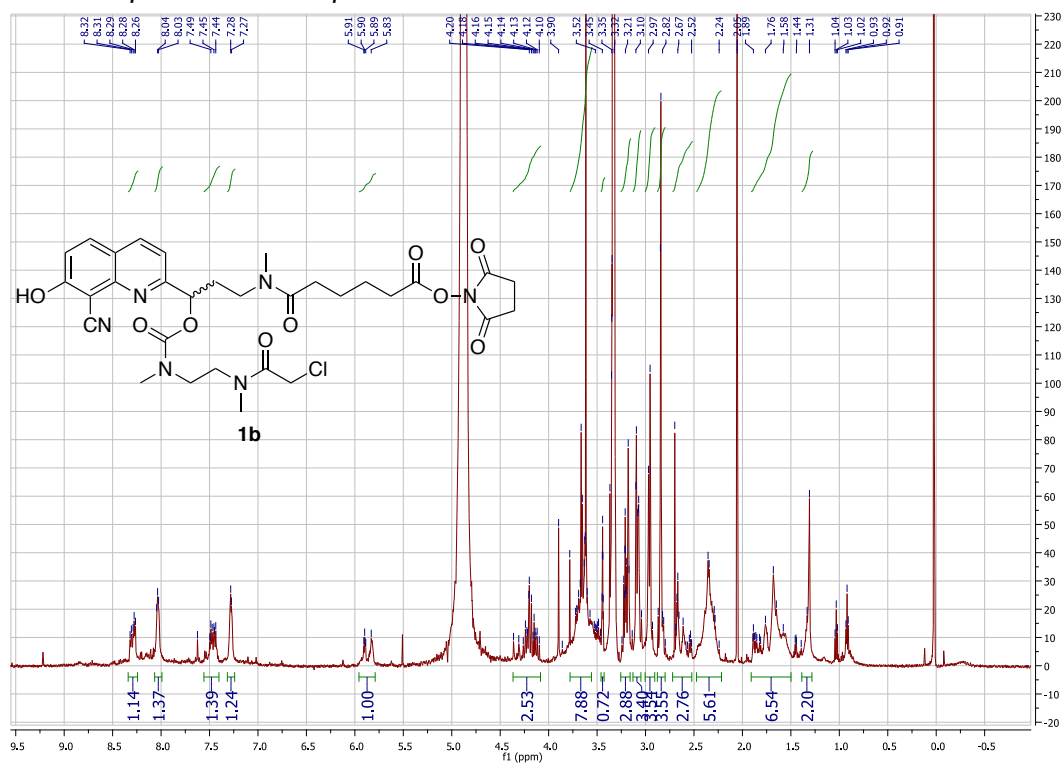


HPLC chromatogram of compound **14**.

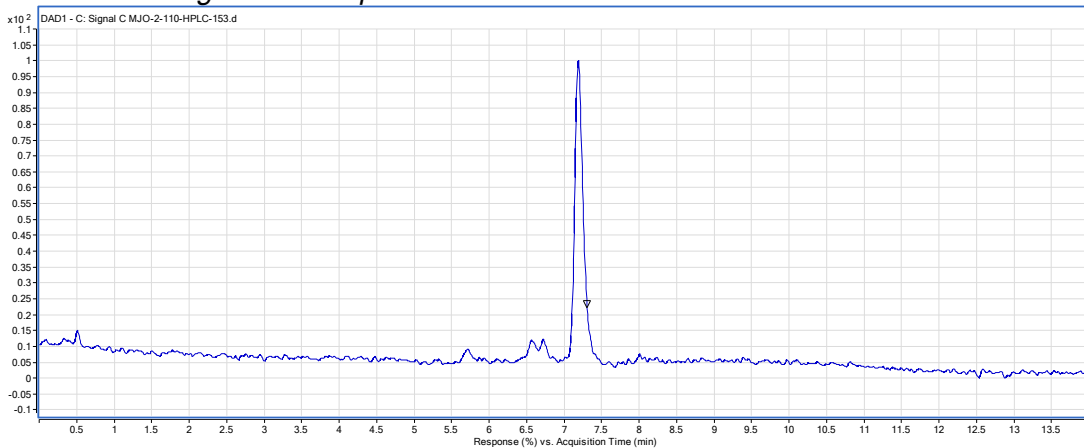


Method: 0-10 min, 5-100% acetonitrile/H₂O, 10-12 min 100% acetonitrile, monitor at 230 nm

¹H NMR spectrum of compound **1b**.

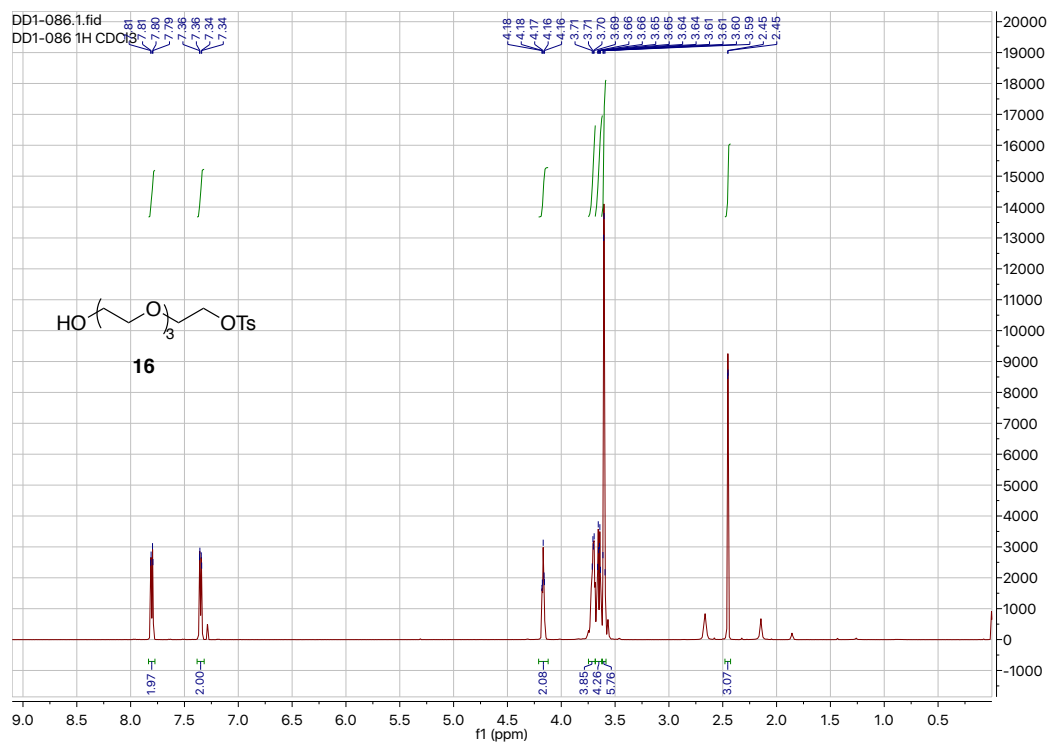


HPLC chromatogram of compound **1b**.

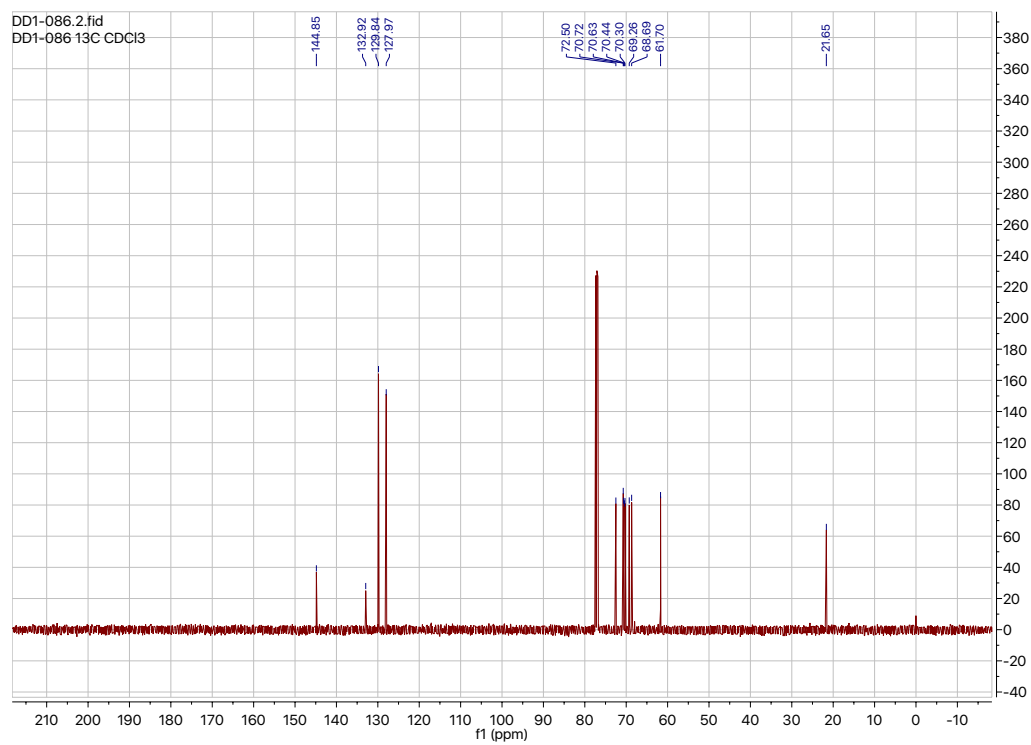


Method: 0-10 min, 5-100% acetonitrile/H₂O, 10-12 min 100% acetonitrile, monitor at 230 nm

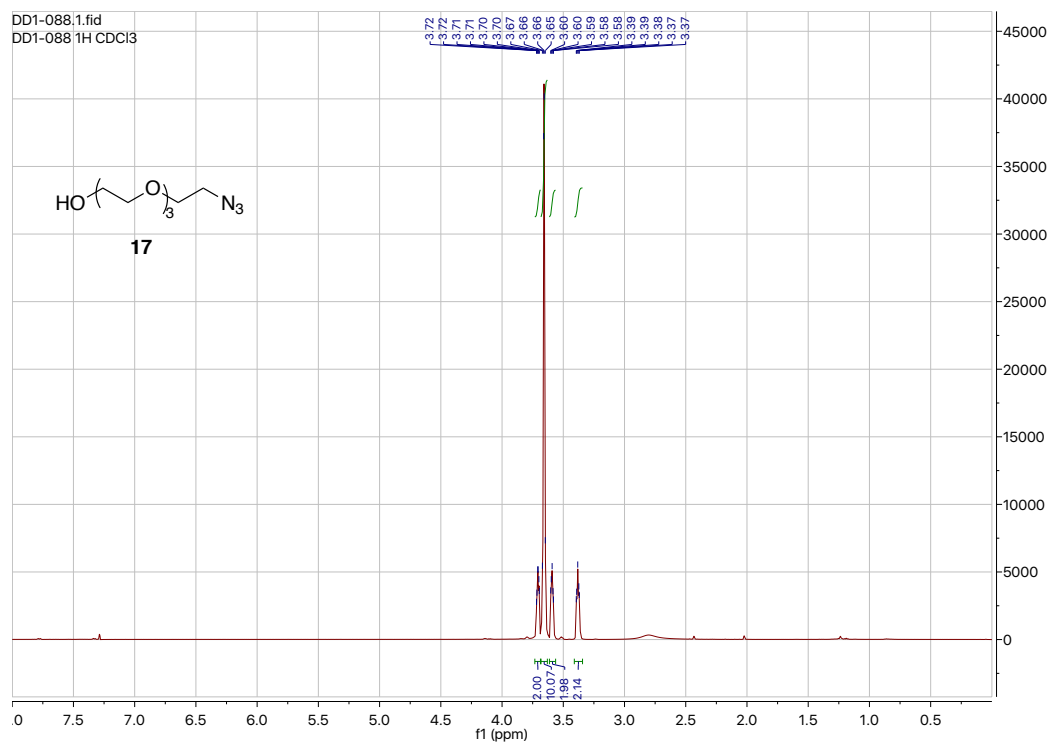
¹H NMR spectrum of compound **16**.



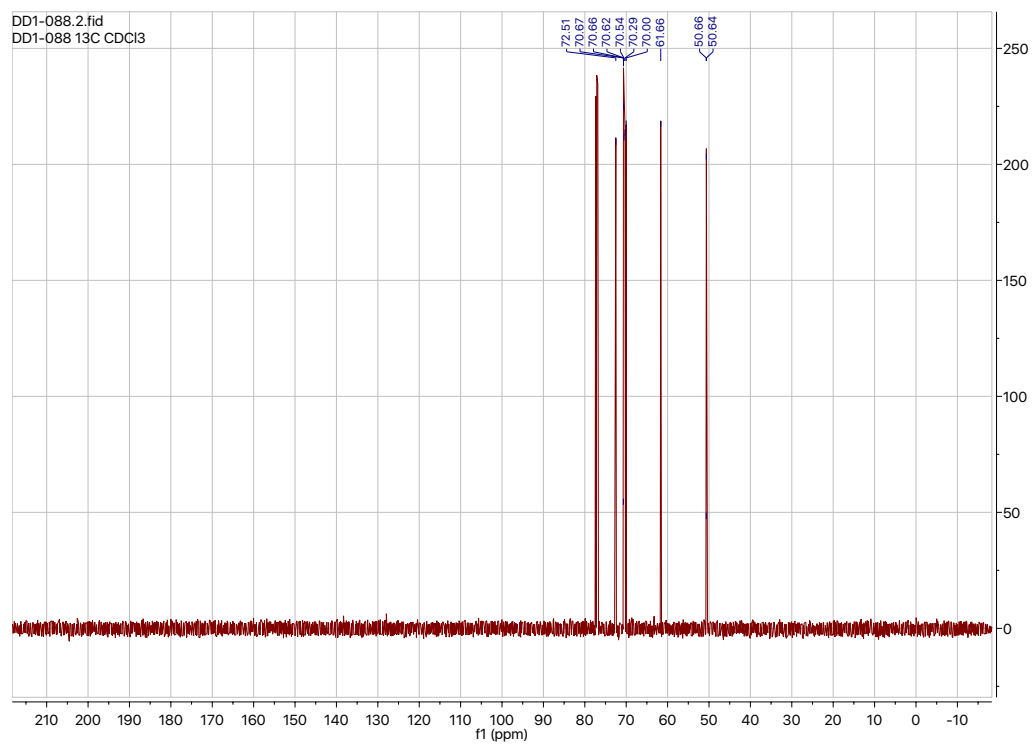
¹³C NMR spectrum of compound **16**.



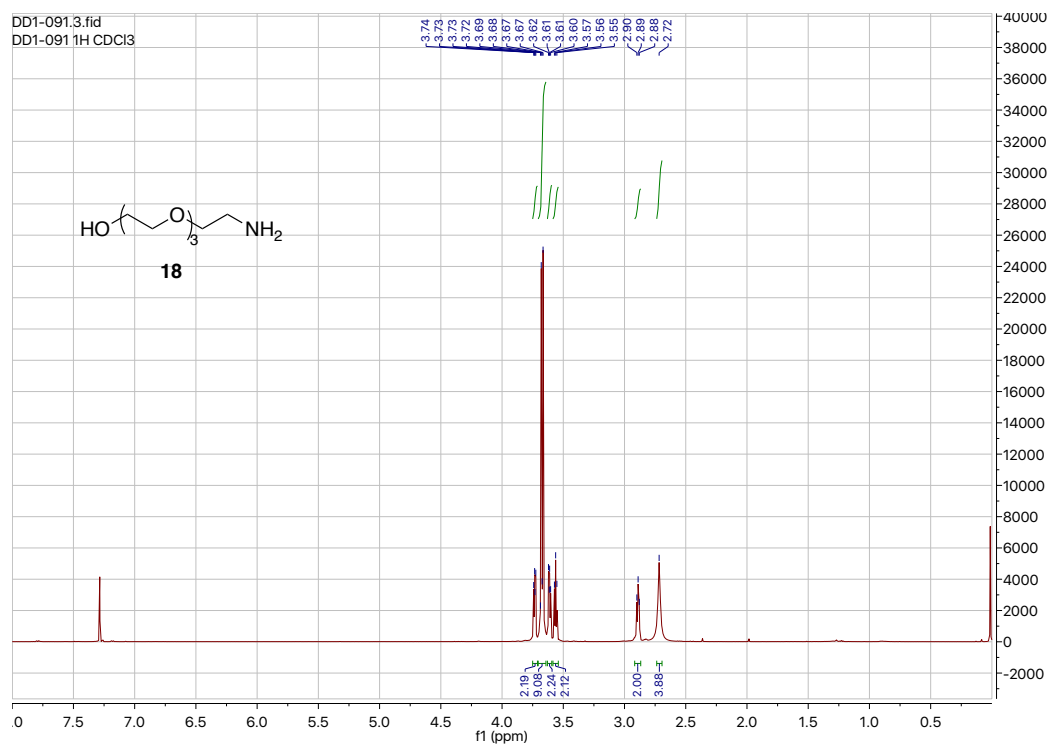
¹H NMR spectrum of compound 17.



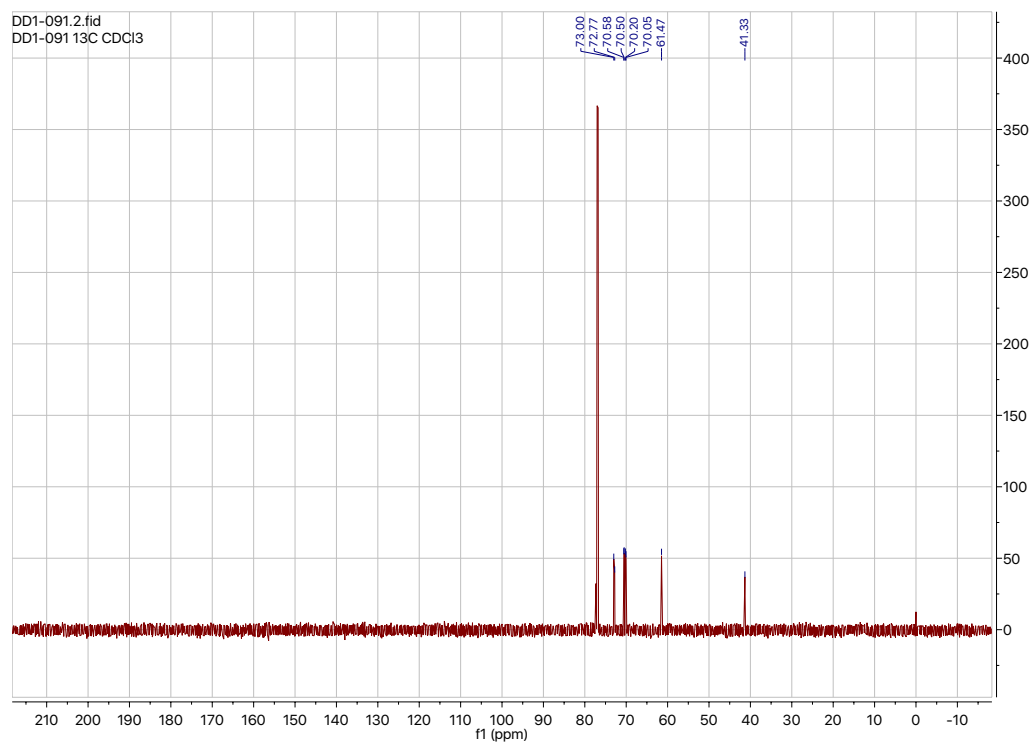
¹³C NMR spectrum of compound 17.



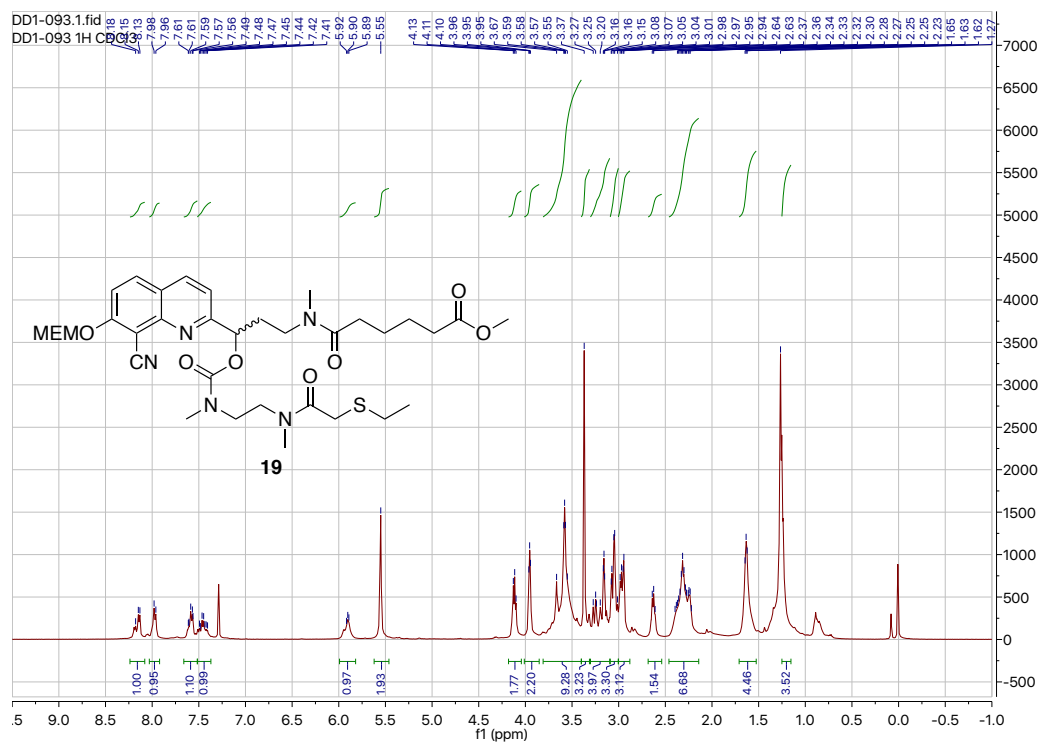
¹H NMR spectrum of compound **18**.



¹³C NMR spectrum of compound **18**.



¹H NMR spectrum of compound **19**.



UV-vis Spectra

UV-vis spectra were recorded on a Thermo Scientific NanoDrop 2000c spectrophotometer with a spectral window measuring from 200 to 800 nm. Single drops of aqueous solution of substrates were analyzed versus drops of blank solution obtaining the final absorbance spectrum. The measurement was repeated in triplicate and the absorbencies averaged. Final ϵ values at λ_{\max} and $\lambda = 405$ nm were obtained from the Beer-Lambert law: $\epsilon = A(c\ell)^{-1}$.

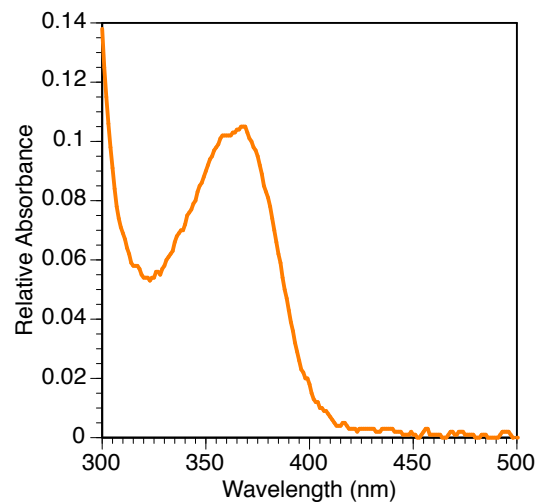


Figure S1. UV-vis spectrum of CyHQ-*gad1b*-cMO (**4b-1**) in water.

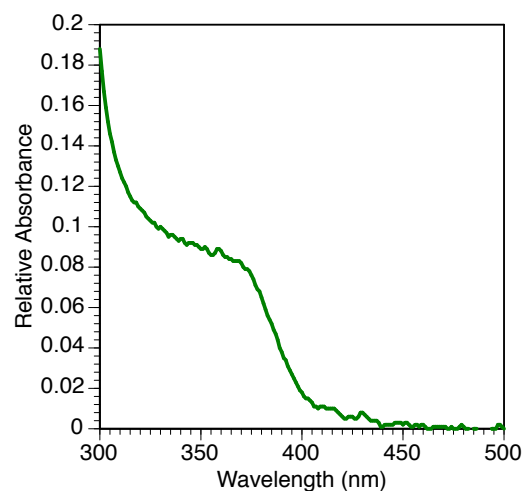


Figure S2. UV-vis spectrum of CyHQ-*gad2*-cMO (**4b-2**) in water.

Photochemistry

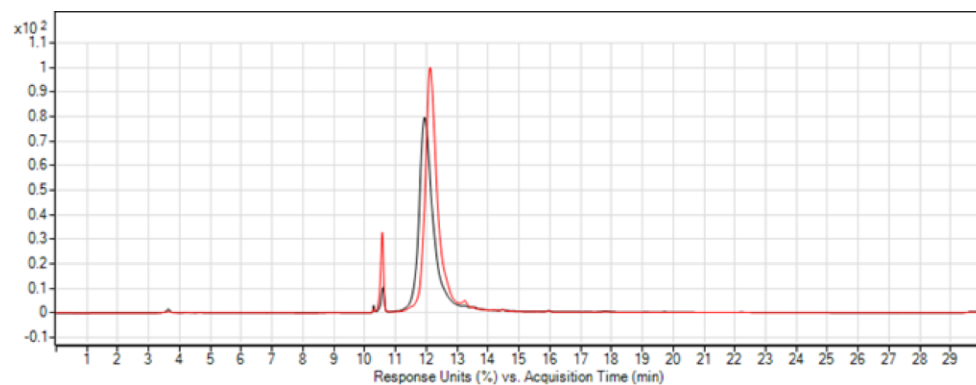


Figure S3. Superimposition of the HPLC traces of CyHQ-*gad1b*-cMO (**4b-1**) before (red line) and after photolysis (black line).

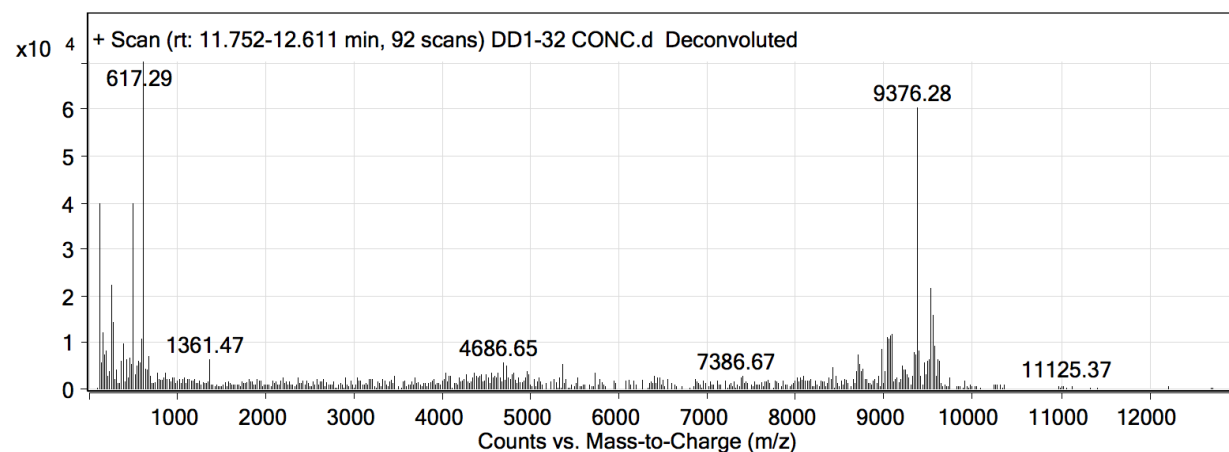


Figure S4. Deconvoluted MS trace of CyHQ-*gad1b*-cMO (**4b-1**) prior to photolysis.

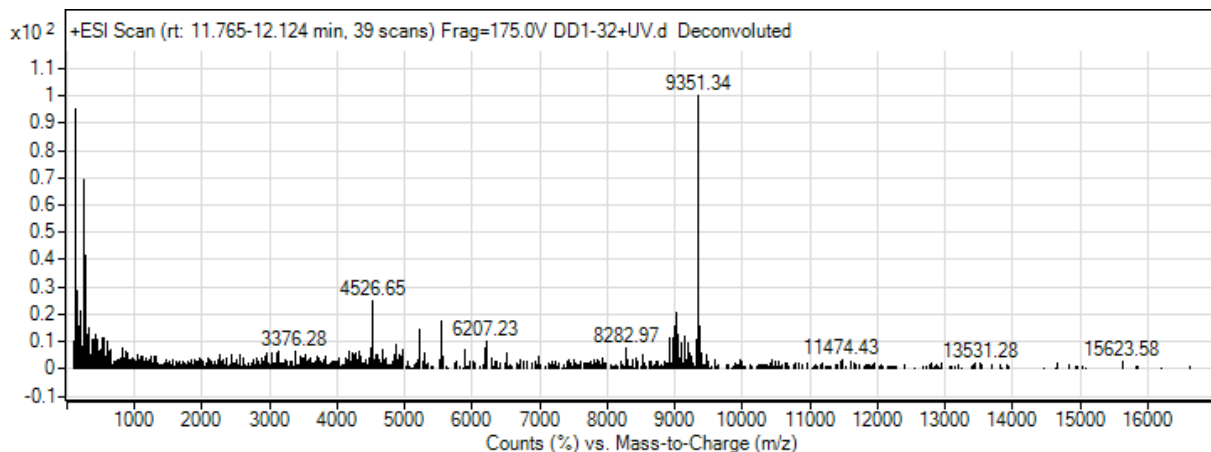


Figure S5. Deconvoluted MS trace of CyHQ-*gad1b*-cMO (**4b-1**) after photolysis.

Stability Toward Enzymatic Degradation

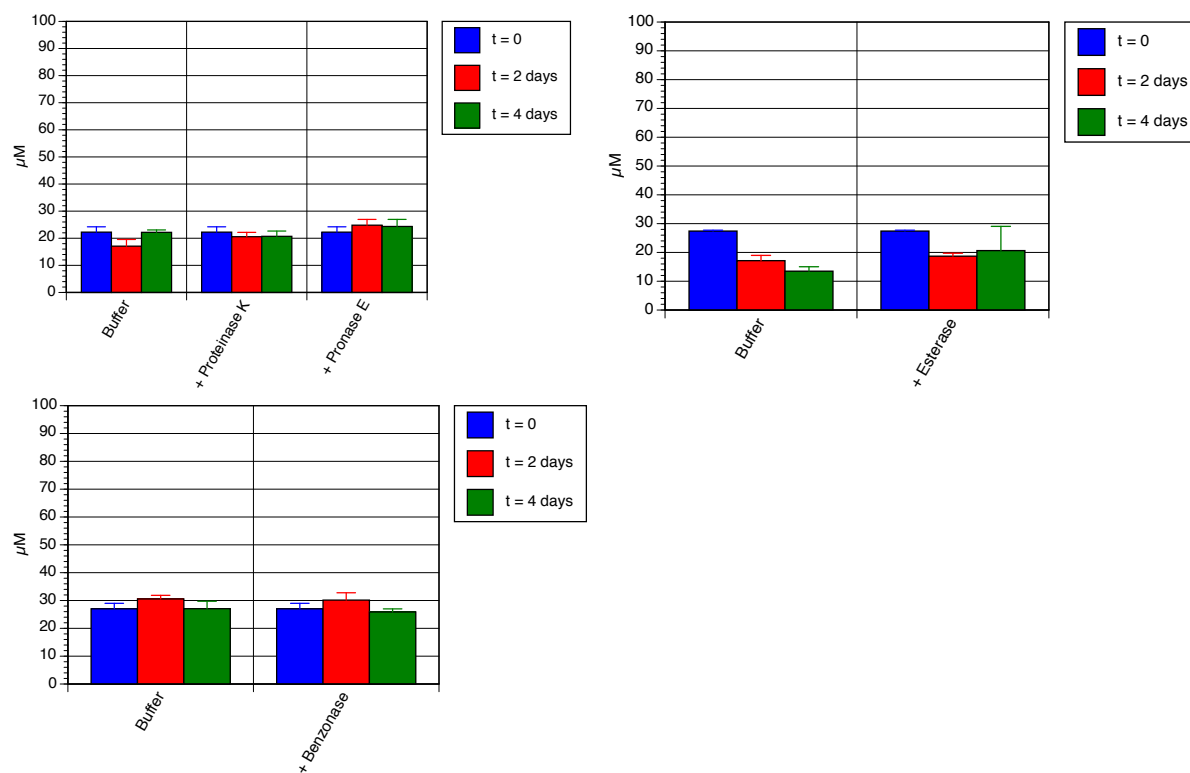


Figure S6. Enzymatic Stability of CyHQ-gad2-cMO (**4b-2**).

Graphs show concentration remaining of **4b-2** as determined by LC-MS/MS. Each experiment was repeated in triplicate. Error bars represent the standard deviation of the measurement. Buffer for proteinase K and pronase E was Tris (50 mM), CaCl₂ (5 mM), pH 7.8; for esterase was borate (10 mM), pH 8.0; and for benzonase was Tris (20 mM), MgCl₂ (2 mM), NaCl (20 mM), pH 8.0.

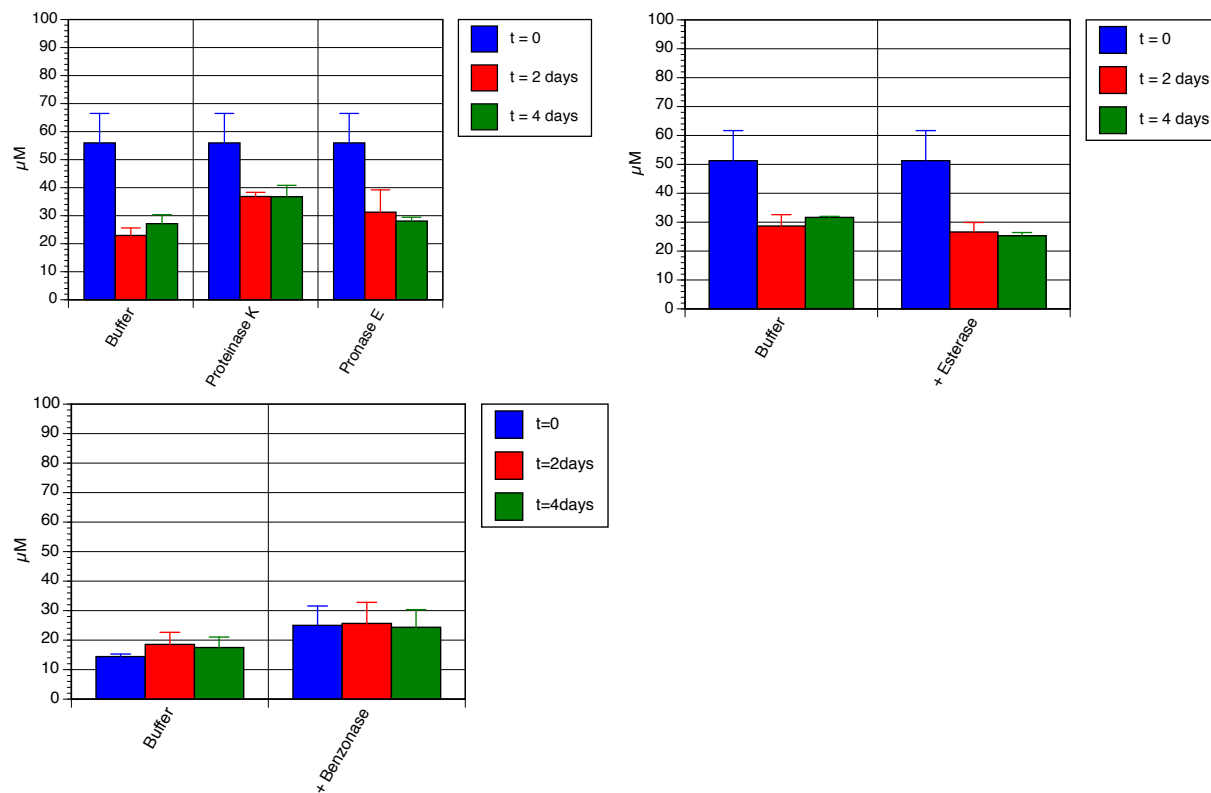


Figure S7. Enzymatic Stability of *gad2*-MO (2-2).

Graphs show concentration remaining of **2-2** as determined by LC-MS/MS. Each experiment was repeated in triplicate. Error bars represent the standard deviation of the measurement. Buffer for proteinase K and pronase E was Tris (50 mM), CaCl_2 (5 mM), pH 7.8; for esterase was borate (10 mM), pH 8.0; and for benzonase was Tris (20 mM), MgCl_2 (2 mM), NaCl (20 mM), pH 8.0.

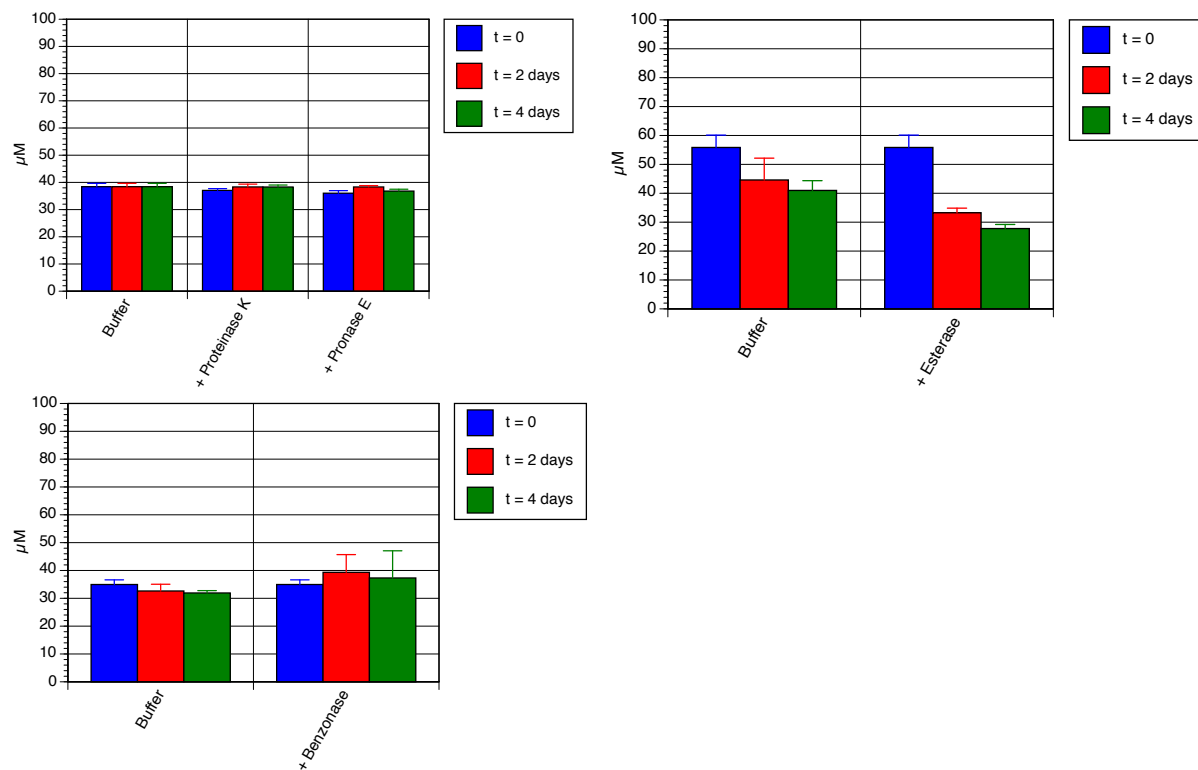


Figure S8. Enzymatic Stability of CyHQ-linker-PEG (**21**).

Graphs show concentration remaining of **21** as determined by LC-MS/MS. Each experiment was repeated in triplicate. Error bars represent the standard deviation of the measurement. Buffer for proteinase K and pronase E was Tris (50 mM), CaCl₂ (5 mM), pH 7.8; for esterase was borate (10 mM), pH 8.0; and for benzonase was Tris (20 mM), MgCl₂ (2 mM), NaCl (20 mM), pH 8.0.

Zebrafish Studies

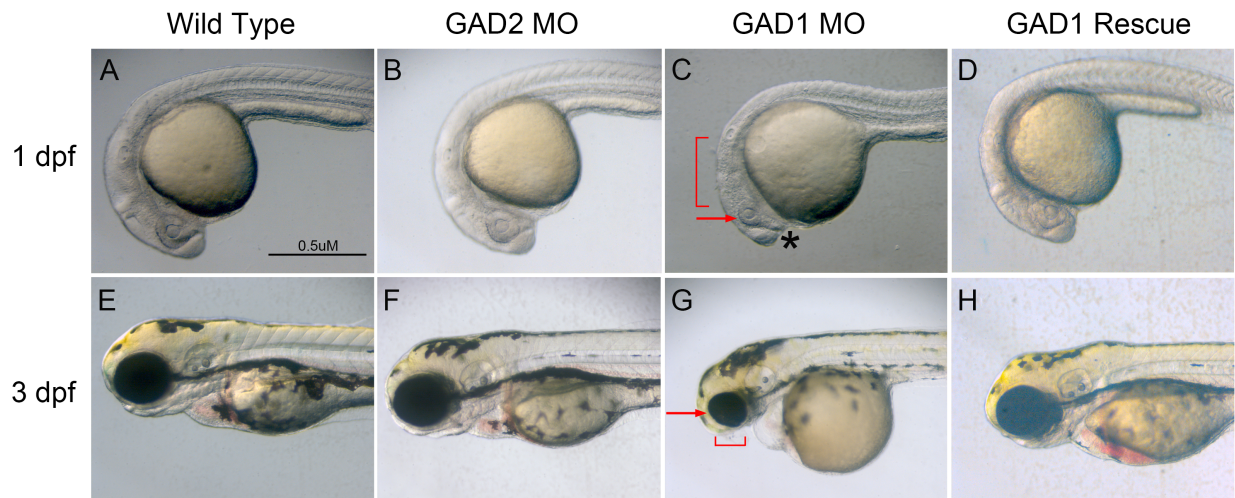


Figure S9. MO knockdown of *gad1b*, but not *gad2* causes morphological defects in craniofacial development.

(A-D) Wild-type, *gad2* morphant (translation blocking MO), *gad1b* morphant (translation blocking MO) and *gad1b* rescue animals at 1 dpf; (E-H) Wild-type, *gad2* morphant, *gad1b* morphant and *gad1b* rescue animals at 3 dpf. (A,B) 1 dpf wild-type and *gad2* morphant animals exhibit comparable morphological development. (C) At 1 dpf *gad1b* morphants exhibit smaller eyes (arrow), an altered distribution of the presumptive head mesenchyme (asterisk), which give the telencephalon a slightly protruding or bulbous appearance, and an altered gross structure of the midbrain-hindbrain region (bracket). (G) At 3 dpf, *gad1b* morphant embryos exhibit abnormal development of the presumptive lower jaw (region denoted by bracket). (D, H) More normal development was observed in embryos in which *gad1b* translation-blocking MOs were co-injected with 0.05 ng synthetic *gad1b* mRNA immune to the MO.

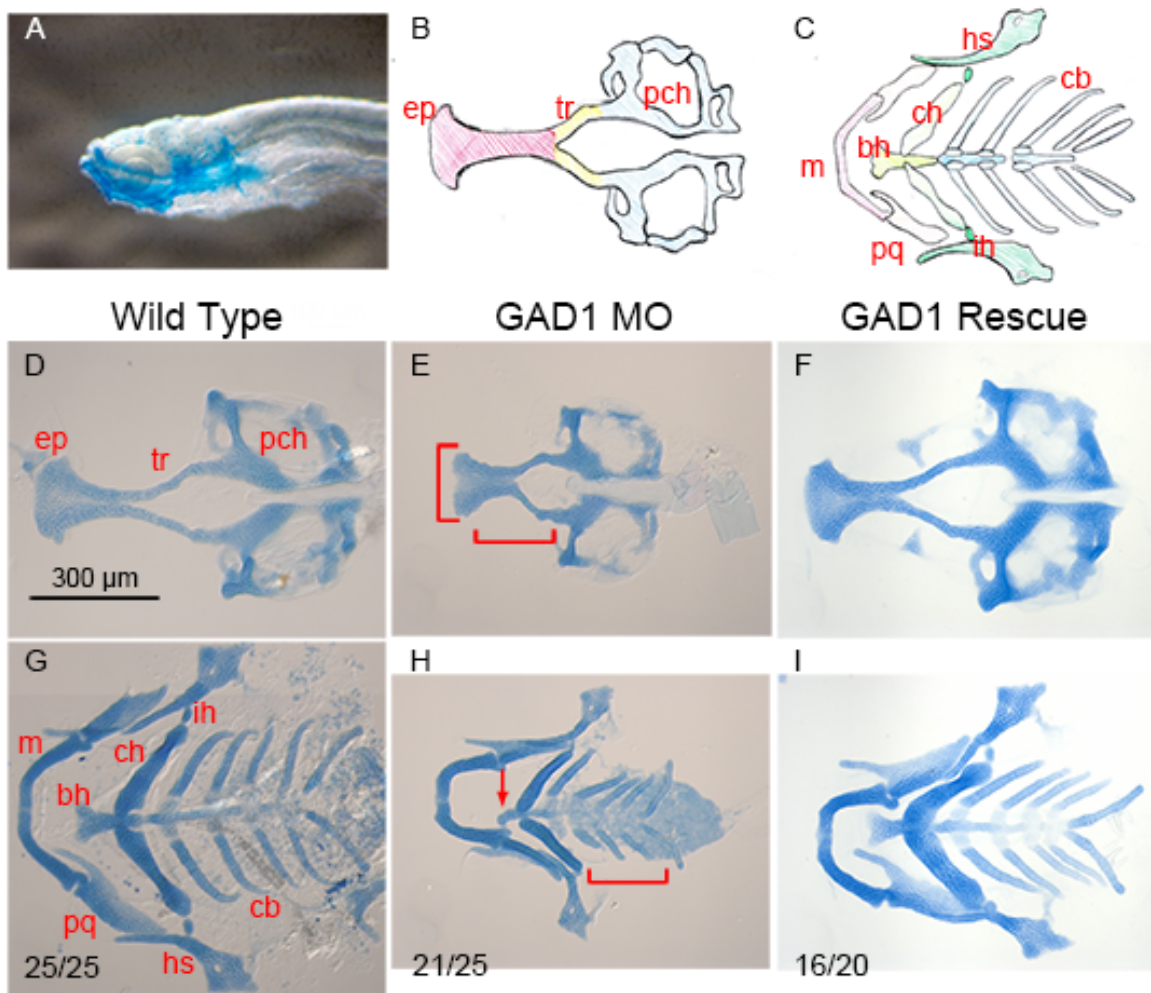


Figure S10. MO knockdown of *gad1b* correlates with smaller, abnormally developed cranial cartilages in flat-mounted samples.

(A) Lateral view of 7 dpf wild-type alcian stained animal; (B) Cartoon of neurocranial structures present at 7 dpf; (C) Cartoon of viscerocranial structures present at 7 dpf; (D-H) Flat mounted samples of cranial cartilages at 7 dpf. (D,G) Wild-type cranial cartilages show normal morphology; (E,H) Cranial cartilages of *gad1b* morphants (translation blocking MO) are significantly smaller than wild-type; (F,I) *gad1b* mRNA (0.05 ng) is sufficient to rescue the small, abnormally shaped cartilage associated with *gad1b* knockdown using a translation blocking MO. (E) *gad1b* morphants exhibit an abnormally shaped ethmoid plate (vertical bracket) and truncated trabeculae (horizontal bracket); (H) *gad1b* morphants display abnormal basihyal cartilage (arrow) and often have truncated ceratobranchial structures (bracket). (bh) basihyal; (cb) ceratobranchial; (ch) ceratohyal; (ep) ethmoid plate; (hs) hyosymplectic; (ih) interhyal; (m) Meckels; (pch) parachordal; (pq) palatoquadrate; (tr) trabeculae. Scale bar in D applies to all images.

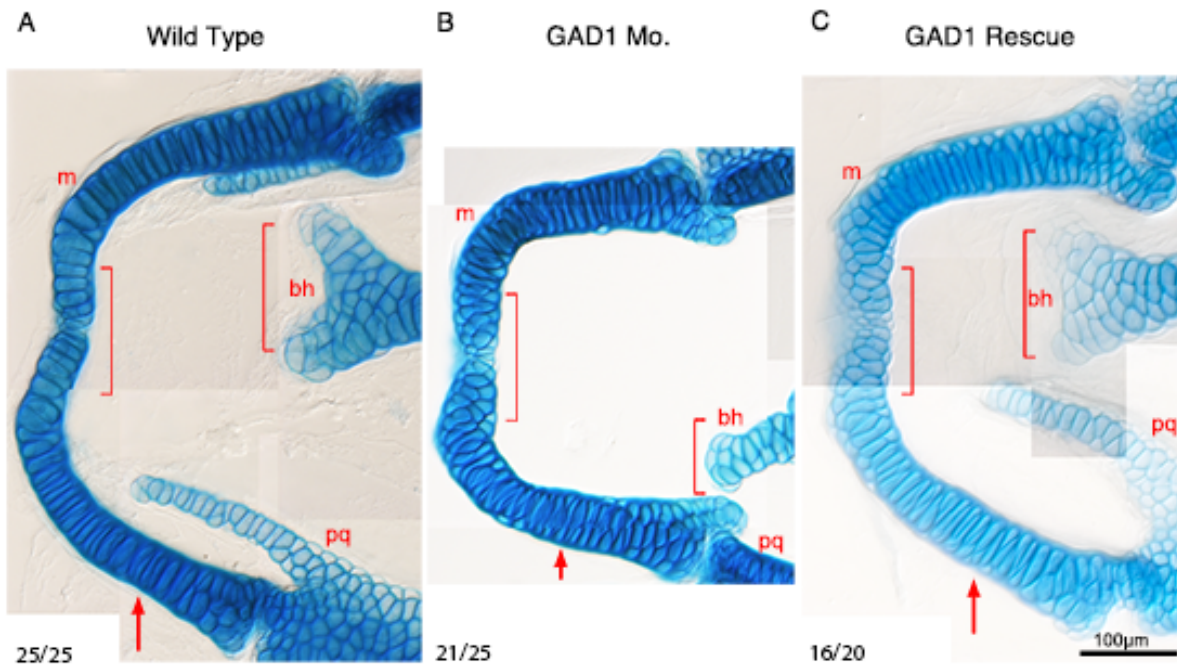


Figure S11. Knockdown of *gad1b* causes aberrant chondrocyte morphology and stacking that can be rescued by co-injection with synthetic *gad1b* mRNA.

(A-C) Flat mounted samples of Meckel's cartilages from 7 dpf animals and imaged at 70x. (A) Wild-type Meckel's cartilage consists of chondrocytes that are elongated and stacked in a planar fashion (arrow). Fusion and elongation points of the Meckel's cartilage and exhibit normal morphology (brackets); (B) *gad1b* morphants display abnormally shaped and aberrant stacking patterns of cranial chondrocytes (arrow). The fusion point of the Meckel's cartilage is thickened due to small, abnormally stacked chondrocytes and the basihyal is misshapen and not fully extended (brackets); (C) Co-injection of *gad1b* translation blocking morpholino and non-targetable, synthetic *gad1b* mRNA (0.05 ng) partially rescues the morphant phenotype. Most chondrocytes regain a normal morphology and stacking pattern, but the midline fusion of the Meckels cartilage retains the abnormal chondrocyte morphology. (bh) basihyal; (m) Meckels; (pq) palatoquadrate. Scale bar in C applies to all images.

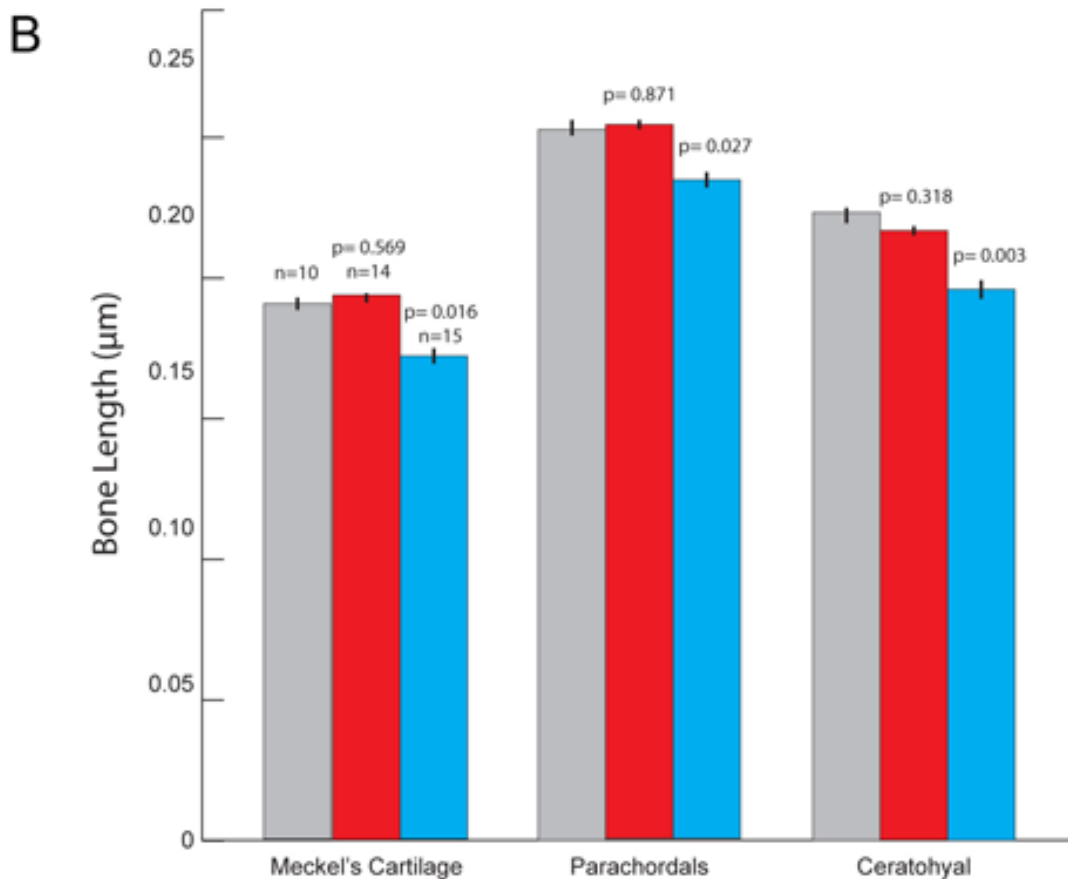
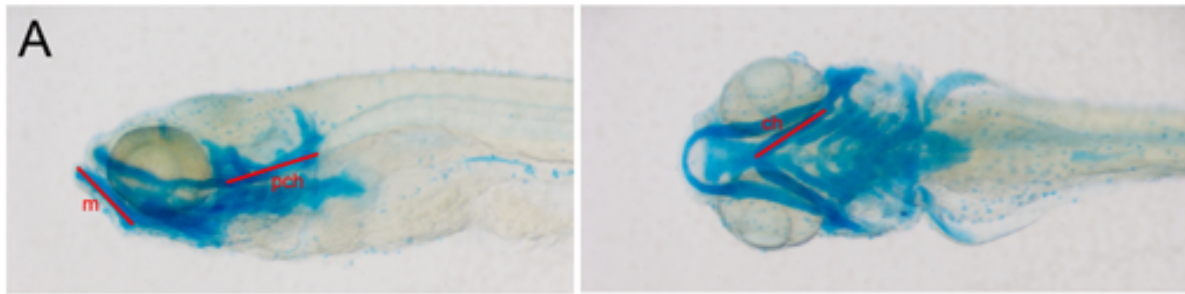


Figure S12. Knockdown of *gad1b*, but not *gad2* leads to smaller cranial cartilages.

(A) Left panel: Lateral view of a wild-type alcian stained animal; Right panel: ventral view of wild-type alcian stained animal. Red lines demarcate where whole-mount measurements were taken; (B) Knockdown of *gad1b* (blue bars) causes Meckel's cartilage, Parachordal cartilage and ceratohyal cartilages to be significantly smaller than in wild-type (grey bars) and *gad2* morphant animals (red bars). Error bars represent SD. (m) Meckel's cartilage; (pch) parachordal cartilage; (ch) ceratohyal cartilage.

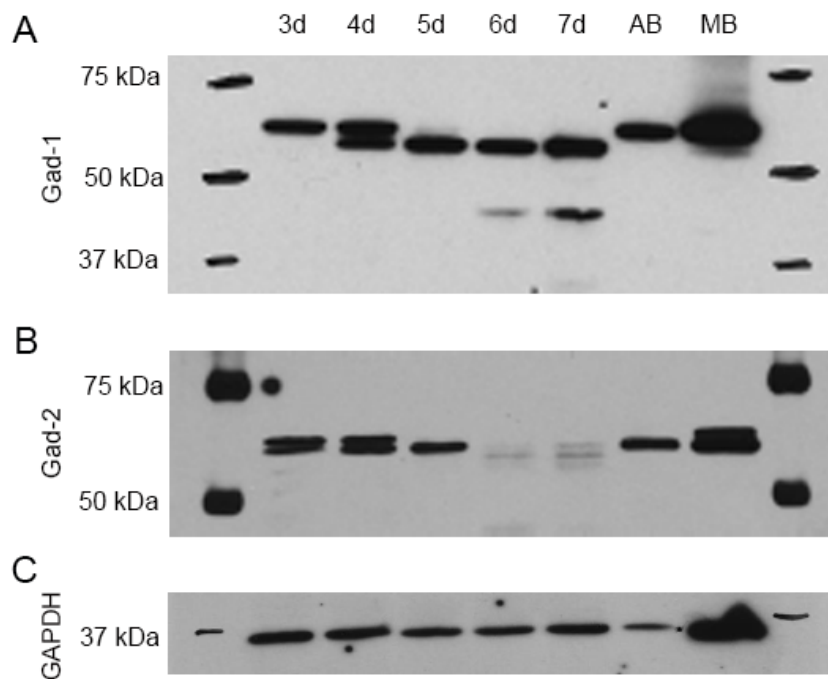


Figure S13. Expression of Gad1 and Gad2 proteins in developing zebrafish.

Protein extracts were prepared from pools of 30-100 zebrafish larvae at 3, 4, 5, 6, and 7 dpf. Protein extracts prepared from adult zebrafish brain (AB) and adult mouse brain (MB) served as positive controls. The same blot was probed for Gad1, Gad2, and GAPDH. Gad1 was detected using a mouse monoclonal to GAD₆₇ (K-87, cat # sc-58531, Santa Cruz Biotechnology Inc), which was raised against amino acids 87-106 (RFRRTETDFS**N**L**F**ARDLLPA) of human GAD₆₇. This antibody reacts with the Gad1b protein in zebrafish; however, it is not yet known if the antibody detects Gad1a (VanLeuven, A. J.; Ball, R. E.; Gunderson, C. E.; Lauderdale, J. D., submitted). The presumptive epitope in Gad1b is R**F****T****R****D****E**TDFS**N**L**F**ARDLLPA and the presumptive epitope in Gad1a is RFRRTETDFS**N**L**Y**ARDLLPA; changes from the human sequence are denoted in bold underline. This antibody does not react with Gad2 protein from zebrafish. Gad2 was detected using a rabbit polyclonal to zebrafish Gad2 (cat #55772, AnaSpec, Inc., Fremont, CA); this antibody does not detect Gad1b (or Gad1a, presumably) in zebrafish. GAPDH served as a loading control. (A) **Gad1**: Three isoforms of Gad1 were detected in zebrafish: an ~67-kDa isoform predominant in extracts prepared from adult zebrafish brain and larvae at 3 and 4 dpf; a ~62 kDa weight isoform predominant in extracts prepared from larvae at 5, 6, and 7 dpf; and a ~44 kDa isoform present in extracts prepared from larvae at 6 and 7 dpf. The 67 kDa isoform was comparable in size to that detected in adult mouse brain. The smaller isoforms are likely due to translation initiating from an internal ATG and/or alternative splicing. (B) **Gad2**: Two isoforms were detected in zebrafish: a ~65 kDa isoform was present in larvae and adult protein extracts; a higher molecular weight isoform was present in larvae at 3 and 4 dpf as well as in mouse brain.


```

          12              24              36              48              60
ATG GCG TCT TCT GCA CCT TCT TCC TCG GCT GGT GAT ATG GAC CCA AAC ACG GCT AAT TTA
Met Ala Ser Ser Ala Pro Ser Ser Ser Ala Gly Asp Met Asp Pro Asn Thr Ala Asn Leu>
_____EXON 2 [Partial]_____>

          72              84              96              108             120
CGA CAA CCT GCC ACA ACC TCG GAC GCG TGG TAC GGG GTT GCA CAC GGA TGC ACG AGG AAA
Arg Gln Pro Ala Thr Thr Ser Asp Ala Trp Tyr Gly Val Ala His Gly Cys Thr Arg Lys>
___EXON 2_____>
_____EXON 3_____>

          132             144             156             168             180
CTG GGC ATG AAG ATC TGT GGT TTC CTG CAG AAG AAC AAC AGT TTG GAT GAG AAG AGT CGT
Leu Gly Met Lys Ile Cys Gly Phe Leu Gln Lys Asn Asn Ser Leu Asp Glu Lys Ser Arg>
_____EXON 3_____>
_____EXON 4_____>

          192             204             216             228             240
ATG GTG GGC TCC TTC AAG GAG AGC GCC AAG AAC CAG ATG TCG TGC GAC AAC AAT GAG CGC
Met Val Gly Ser Phe Lys Glu Ser Ala Lys Asn Gln Met Ser Cys Asp Asn Asn Glu Arg>
_____EXON 4_____>

          252             264             276             288             300
TTC ACG CGC GAT GAG ACA GAT TTC TCC AAC CTG TTC GCG CGA GAT CTA CTG CCC GCT AAA
Phe Thr Arg Asp Glu Thr Asp Phe Ser Asn Leu Phe Ala Arg Asp Leu Leu Pro Ala Lys>
_____EXON 4_____>
_____EXON 5_____>

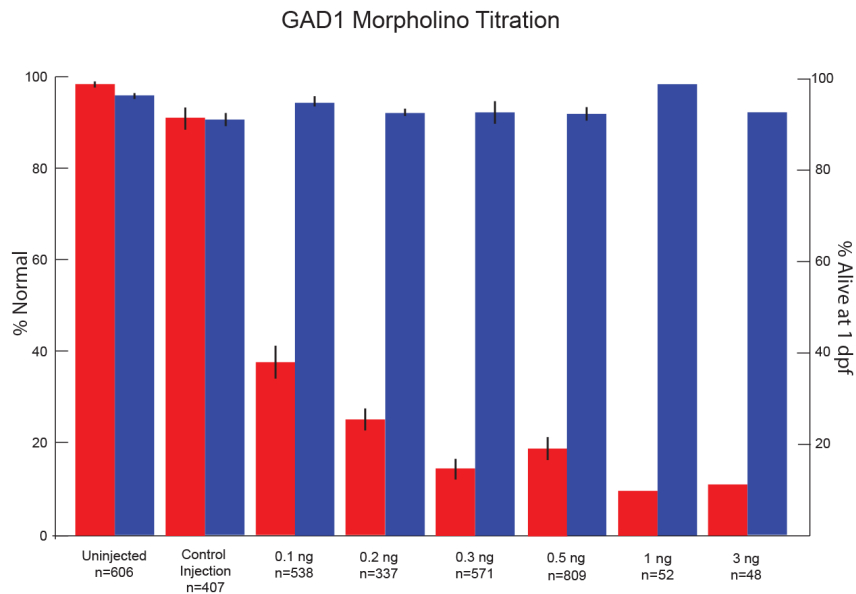
```

Met position	Exon	Predicted MW kDa (no alt splicing)
1	2	66155.38
13	2	65106.30
43	3	61891.73
61	4	59798.29
73	4	58490.81

Figure S14. Sequence of *gad1b* exons 2 through 4.

To provide standardized coordinates,³ the first base of the ATG initiation codon in the *gad1b* cDNA reference sequence is denoted as nucleotide 1, and the first methionine is denoted as M₁. ATG codons located upstream of the anti-GAD₆₇ epitope (denoted in bold) are highlighted in yellow; the location of each is given relative to M₁ in the full-length protein. The predicted molecular weights of hypothetical Gad1b proteins associated with translation initiation from each ATG in exons 2 through 4 are shown in the associated table.

A



B

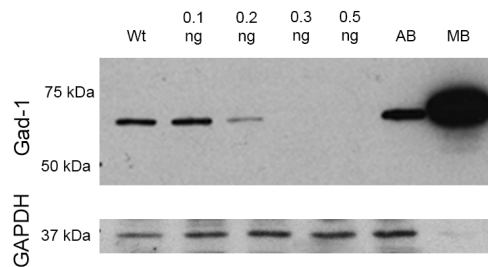


Figure S15. Titration of *gad1b* translation blocking morpholino.

(A) Red bars represent percent of injected animals that exhibited normal morphology at 1 dpf as determined by visual inspection under a microscope, and blue bars represent the percent of injected animals alive at 1 dpf. The total number of injected embryos obtained from 5-7 independent experiments is given for controls and *gad1b* MO amounts equal to or less than 0.5 ng. A single injection set was performed for *gad1b* MO amounts of 1 ng and 3 ng. Error bars represent SEM. Embryos in the control injection set received injection buffer only. (B) Western blot analysis of Gad1 protein in pools of embryos injected with different amounts of *gad1b* MO. Protein extracts were prepared from 30-100 embryos at 3 dpf per given MO dose. Blots were probed using a mouse monoclonal to GAD₆₇ (K-87, cat # sc-58531, Santa Cruz Biotechnology Inc.). Protein extracts prepared from WT embryos, adult zebrafish brain (AB) and adult mouse brain (MB) served as positive controls. GAPDH served as a loading control. The optimal dose of *gad1b* MO was determined to be 0.3 ng per embryo (1-nL injection volume × 0.3 ng *gad1b* MO/nL).

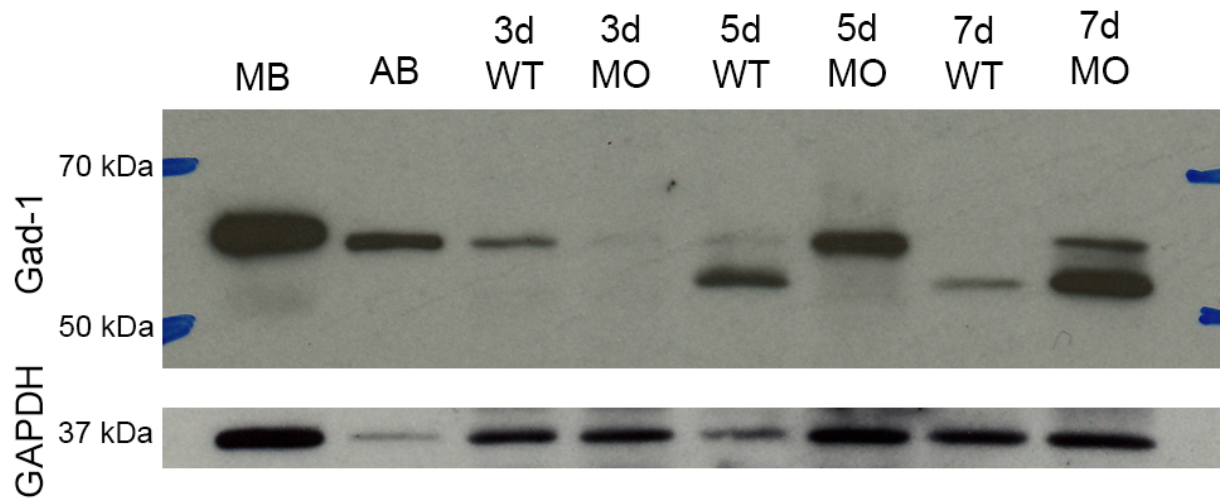
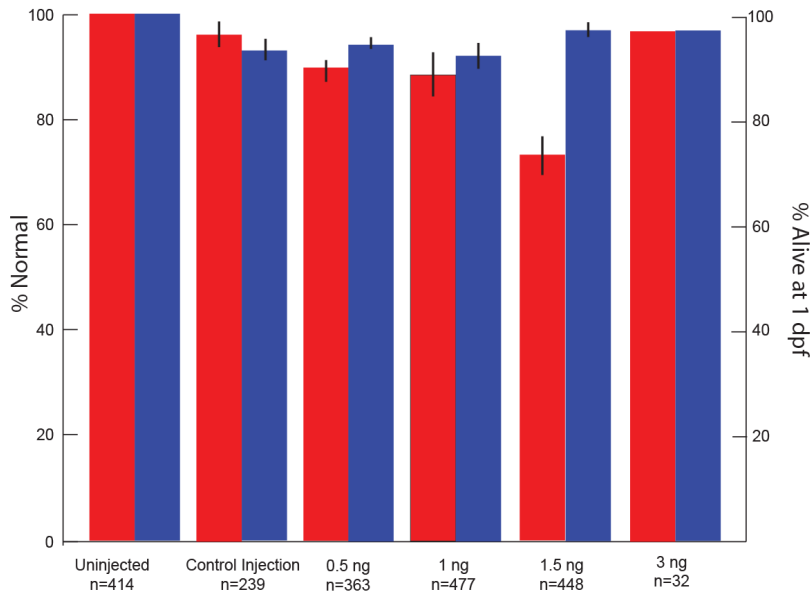
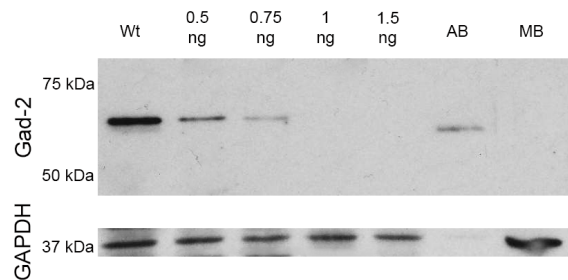


Figure S16. The *gad1b* MO knockdown at 0.3 ng per embryo is effective through 3 dpf.

Western blot analysis of Gad1 protein in pools of zebrafish embryos injected with 0.3 ng *gad1b* translation blocking MO at the 1-4 cell stage. Protein extracts were prepared from 30-100 embryos at 3, 5, and 7 dpf. Blots were probed using a mouse monoclonal to GAD₆₇ (K-87, cat # sc-58531, Santa Cruz Biotechnology Inc.). Protein extracts prepared from WT embryos, adult zebrafish brain (AB) and adult mouse brain (MB) served as positive controls. GAPDH served as a loading control.

A**GAD2 Morpholino Titration****B****Figure S17.** Titration of *gad2* translation blocking morpholino.

(A) Red bars represent percent of injected animals that exhibited normal morphology at 1 dpf as determined by visual inspection under a microscope, and blue bars represent the percent of injected animals alive at 1 dpf. The total number of injected embryos obtained from 5-7 independent experiments is given for controls and *gad2* MO amounts equal to or less than 1.5 ng. A single injection set was performed for *gad2* MO amounts of 3 ng. Error bars represent SEM. Embryos in the control injection set received injection buffer only. (B) Western blot analysis of Gad2 protein in pools of embryos injected with different amounts of *gad2* MO. Protein extracts were prepared from 30-100 embryos at 3 dpf per given MO dose. Blots were probed using a rabbit polyclonal to zebrafish Gad2 (cat #55772, AnaSpec, Inc., Fremont, CA). Protein extracts prepared from adult zebrafish brain (AB) and WT embryos served as positive controls; protein extract prepared from adult mouse brain (MB) was included to test species specificity. GAPDH served as a loading control. The optimal dose of *gad2* MO was determined to be 1 ng per embryo (1-nL injection volume x 1.0 ng *gad2* MO/nL).

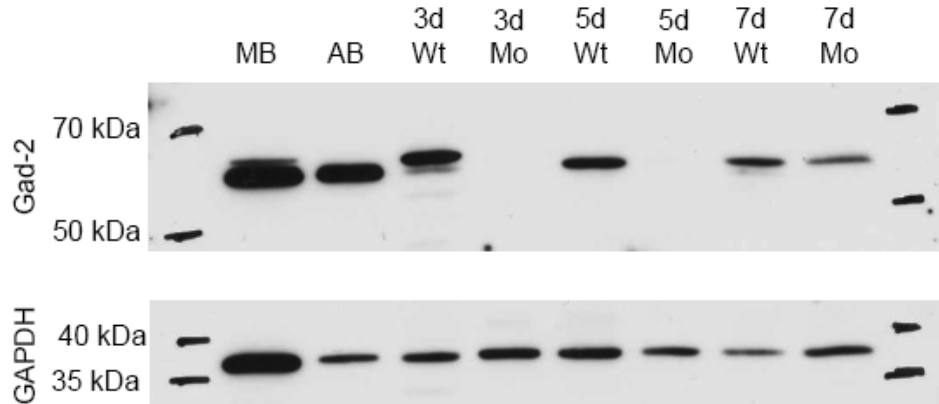


Figure S18. The *gad2* MO knockdown at 1 ng per embryo is effective through 5 dpf.

Western blot analysis of Gad2 protein in pools of zebrafish embryos injected with 1 ng *gad2* translation blocking MO at the 1-4 cell stage. Protein extracts were prepared from 30-100 embryos at 3, 5, and 7 dpf. Blots were probed using a rabbit polyclonal to zebrafish Gad2 (cat #55772, AnaSpec, Inc., Fremont, CA). Protein extracts prepared from WT embryos and adult zebrafish brain (AB) served as positive controls; protein extract prepared from adult mouse brain (MB) was included to test species specificity. GAPDH served as a loading control. Under these conditions, the *gad2* MO was effective at blocking translation of the Gad2 protein through 5 dpf.

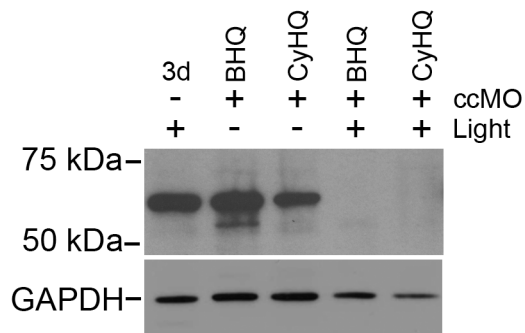


Figure S19. Western blot analysis of BHQ-*gad1b*-ccMO and CyHQ-*gad1b*-ccMO.

Western blot analysis of Gad1 protein in pools of zebrafish embryos injected at the 1-4 cell stage with 0.5 ng BHQ-*gad1b*-ccMO or CyHQ-*gad1b*-ccMO under red-light conditions. One half of each pool was then exposed to light to uncage the ccMOs. All fish were then raised to 3 dpf under the same conditions. Protein extracts were prepared from 15-30 embryos per injection set at 3 dpf and quantitated using the bicinchoninic acid (BCA) assay (Pierce). Equal amounts of extract were loaded in each lane. Blots were probed using a mouse monoclonal to GAD₆₇ (K-87, cat # sc-58531, Santa Cruz Biotechnology Inc.). The blot was stripped and reprobed for GAPDH. Protein extracts prepared from uninjected embryos served as controls.

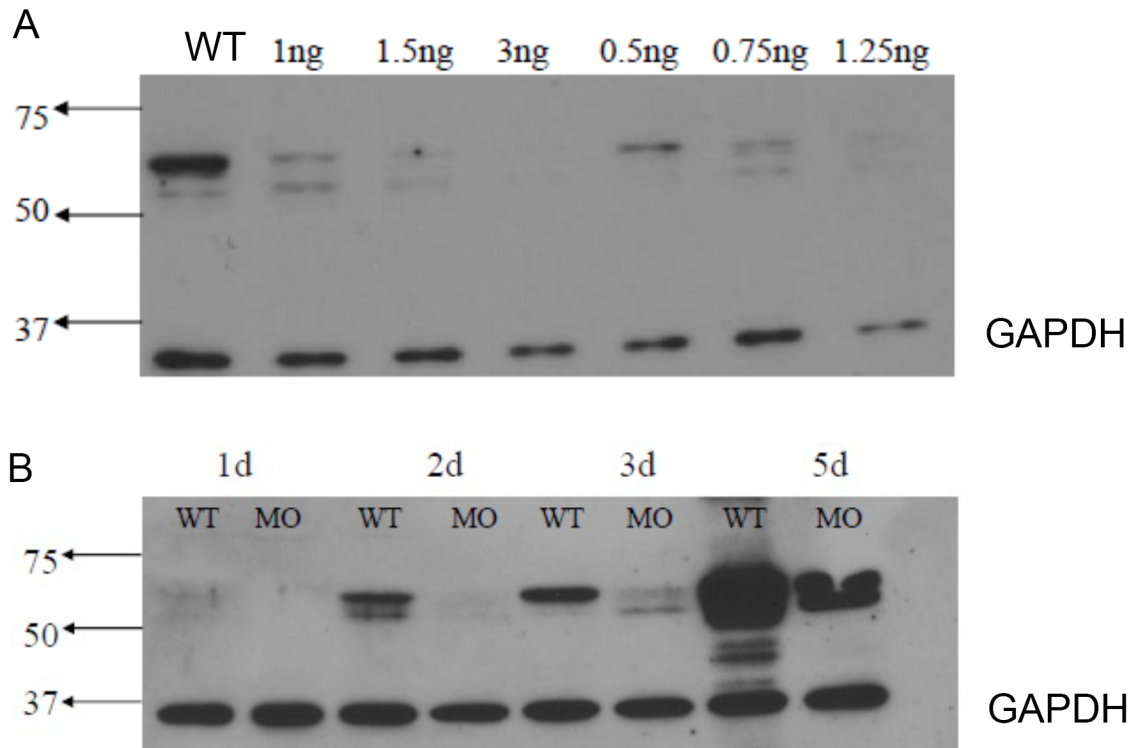


Figure S20. Western blot analysis of *gad1b* splice blocking morpholino.

(A) Titration of *gad1b* splice blocking MOs assessed at 3 dpf. (B) The *gad1b* splice blocking MO at 1.25 ng is effective through 3 dpf. Western blot analysis of Gad1 protein in pools of zebrafish embryos injected at the 1-4 cell stage with *gad1b* splice blocking MO. Protein extracts were prepared from 15-30 embryos per injection set and quantitated using the bicinchoninic acid (BCA) assay (Pierce). Equal amounts of extract were loaded in each lane. Blots were probed using a mouse monoclonal to GAD₆₇ (K-87, cat # sc-58531, Santa Cruz Biotechnology Inc.) and a rabbit polyclonal to GAPDH (ab9484, Abcam, Cambridge, MA). Protein extracts prepared from uninjected embryos served as controls.

Design of Splice Blocking Morpholinos. Splice blocking Morpholinos (MO) were designed to bind to the exon 2-intron 2 junction of *gad1b* and the exon 3- intron 3 junction of *gad2*. The first translation initiation codon for *gad1b* is in exon 2, and the translation initiation codon for *gad2* is located in exon 1. Five base mismatch controls were used. The sequences of the MOs are:
gad1b Splice Blocker: 5'-TGTGATTTGTGGTGATTTACCTGTT-3'
gad1b Splice Control: 5' TGTcATTTcTGGTcATTTACgTcTT-3'
gad2 Splice Blocker: 5'-GCGTTATCCAGAGACCTACTTGT-3'
gad2 Splice Control: 5' GCcTTATgCAcAGAcACCTACTTcT-3'

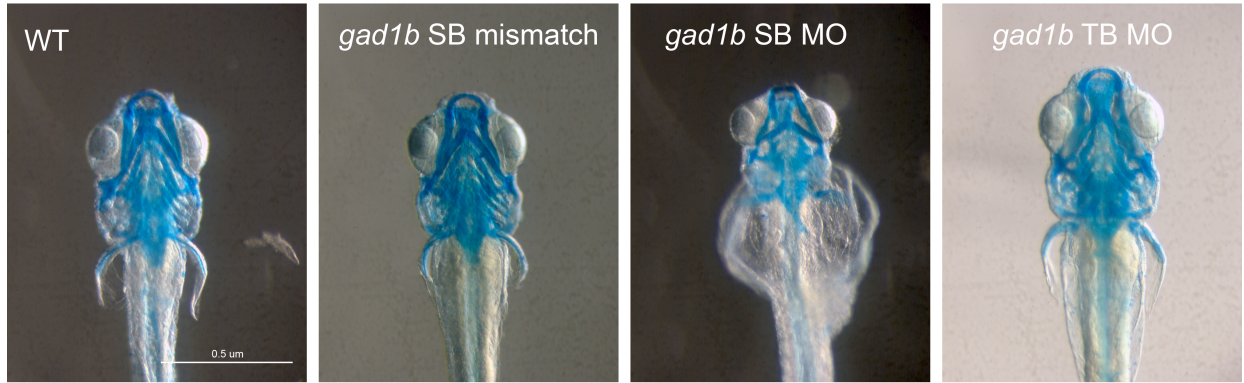


Figure S21. Knockdown of *gad1b* using a splice blocking MO causes morphological defects in the zebrafish head skeleton.

Ventral view of alcian stained larvae at 7 dpf. Embryos injected with *gad1b* splice blocking mismatch control MOs exhibit normal skeletal development (n=14/14). Embryos injected with 1.25 ng of *gad1b* splice blocking MOs exhibit altered cartilage development (n=10/10) comparable or more severe than embryos injected with 0.3 ng *gad1b* translation blocking MO; this fish is comparable to those used to prepare the flat mounts show in Supplemental Figure S10.

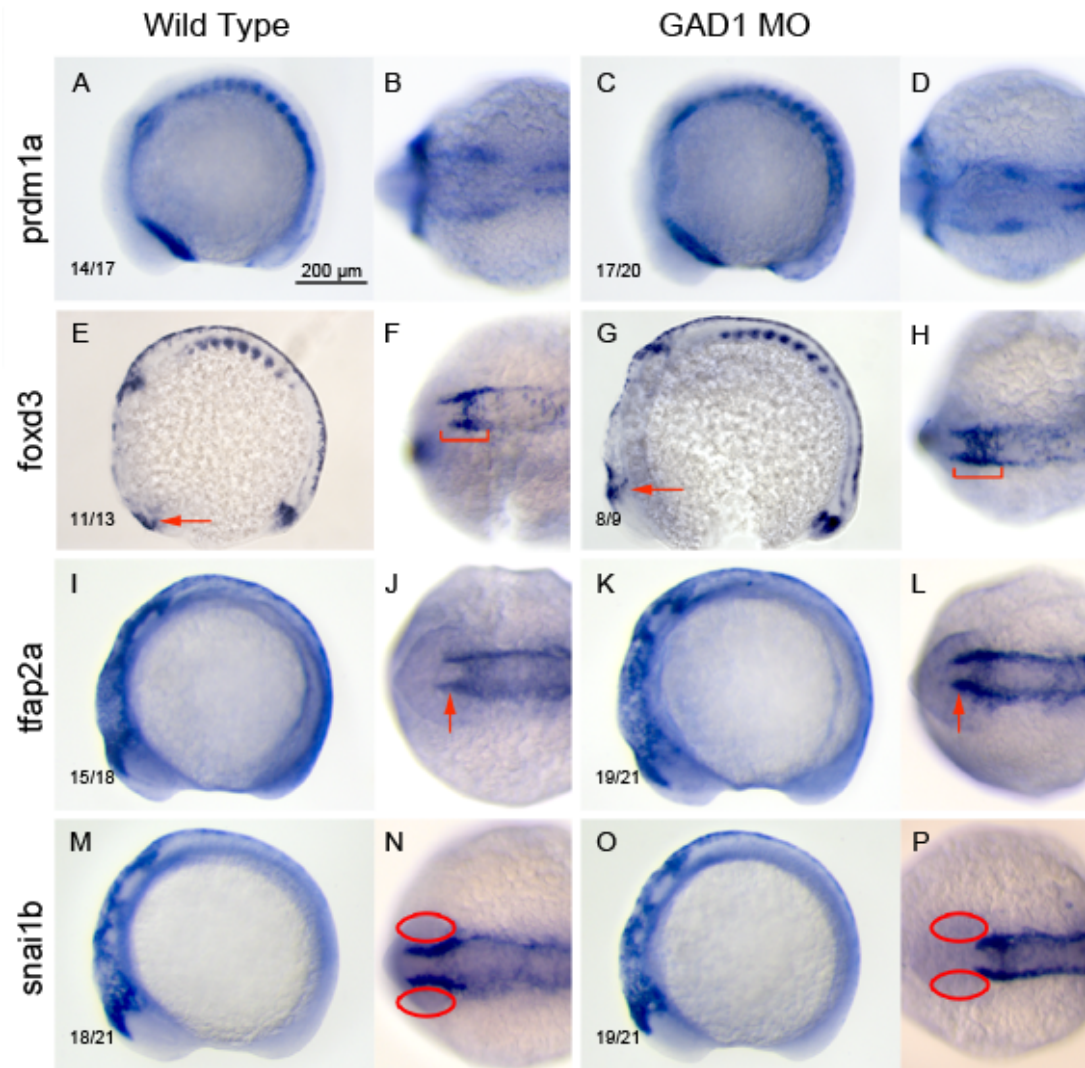


Figure S22. The *gad1b* translation blocking morphants exhibit altered expression of early neural crest markers *foxd3*, *tfap2a*, and *snail1b*.

(A-F) Lateral and dorsal views of wild-type (A,B,E,F,I,J,M,N) and *gad1b* morphant (C,D,G,H,K,L,O,P) embryos at 10-12 somites of development showing expression of *prdm1a* (A-D), *foxd3* (E-H) and *tfap2a* (I-L), and *snail1b* (M-P). Gene expression was assessed by whole-mount mRNA *in situ* hybridization. The head skeleton in zebrafish, as in mammals, develops from cranial neural crest (CNC) cells. In zebrafish, the premigratory neural crest in the head is located lateral to the developing neural keel during the 1- to 10-somite stages (9 through 14 hpf)^{4, 5} and express genes associated with neural crest (e.g., *prdm1a*, *tfap2a*, *foxd3*, *snail1b*).⁵⁻¹⁷ (A-D) The expression of *prdm1a* is comparable to wild-type animals in both trunk and cranial neural crest populations (D); (E-H) the pattern of *foxd3* expression appeared expanded in *gad1b* morphants (compare regions denoted with arrows and bracket between wild-type and morphant embryos); *foxd3* expression is normally downregulated in wild-type embryos upon CNC migration;¹⁴ (I-L) expression of *tfap2a* appears expanded in *gad1b* morphants (arrows); (M-P) *snail1b* expression is diminished in the anterior brain in *gad1b* morphants (circles denote position of eyes).

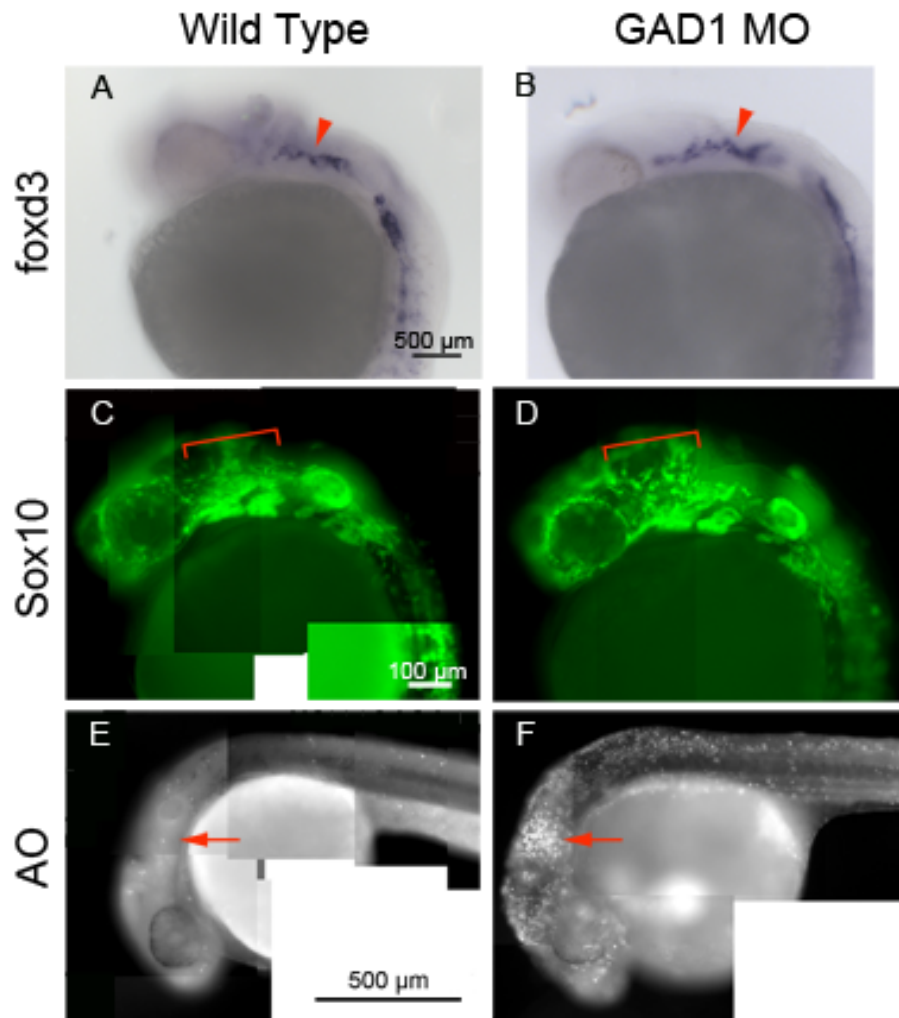


Figure S23. The *gad1b* translation blocking morphants exhibit altered distribution of *foxd3* or *sox10* expressing cells and an increase in acridine orange (AO) staining at 1 dpf.

(A-F) Lateral views of wild-type (A,C,E) and *GAD1* morphants (B,D,F) embryos at 1 dpf, showing expression of *foxd3* as visualized by whole-mount mRNA *in situ* hybridization (A,B), *sox10* as visualized by EGFP reporter gene expression from a *sox10:eGFP* [Tg(-4.9sox10:eGFP)] transgene, which labels chondrogenic neural crest^{18, 19} (C,D) and acridine orange (E,F). Beginning ~15 hpf, CNC cells delaminate from the ectoderm overlying the dorsal neural tube in a wave originating at the midbrain and progressing along in caudal direction and migrate as separate streams into the pharyngeal arches.^{4, 5} The bulk of this migration occurs between 18 and 24 hpf. During migration, these cells continue to proliferate and begin to express genes associated with formation and differentiation of mesenchymal condensations.²⁰⁻²² Neurocranial precursors originate in the midbrain region and migrate between the eyes to form the palatal shelves, and the pharyngeal arches are populated by CNCs that emigrate from the hindbrain.²³ *gad1b* morphants exhibit altered distribution of *foxd3* or *sox10* expressing cells compared to wild-type embryos (compare regions denoted by arrowheads in A and B; brackets in C and D). (E,F) *gad1b* morphants exhibit an increase in the number of apoptotic cells as visualized by acridine orange staining in the head and pharyngeal arch regions (compare regions indicated with arrows).

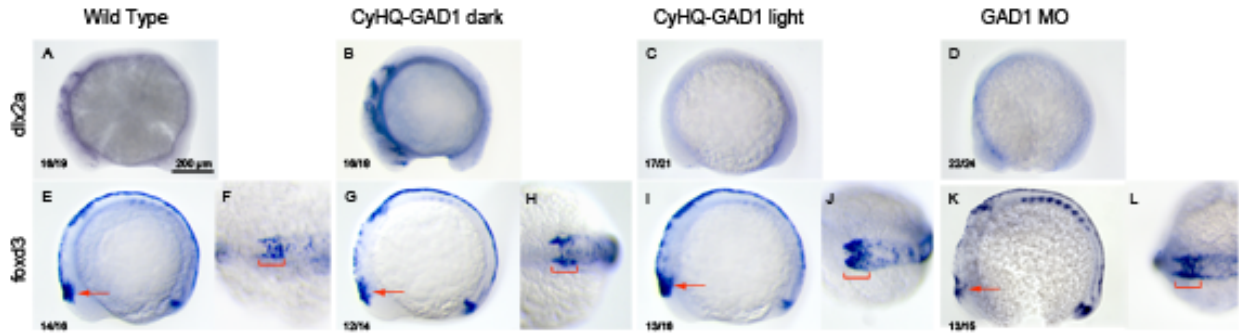


Figure S24. Embryos harboring caged-*gad1b* translation blocking morpholinos exhibit normal expression of early neural crest markers *dlx2a* and *foxd3* at 10-12 somites of development.

Lateral views of embryos showing expression of *dlx2a* in wild-type (A), caged CyHQ-*gad1b*-MO (B), uncaged CyHQ-*gad1b*-MO (C) and *gad1b* MO animals (D). Gene expression was assessed by whole-mount mRNA *in situ* hybridization (ISH). (A,B) Expression of *dlx2a* was comparable between wild-type and CyHQ-*gad1b*-MO injected embryos raised in the dark. (C,D) Expression of *dlx2a* was reduced in *gad1b* morphant animals and comparable reduction was observed in CyHQ-*gad1b*-MO morphants where the morpholino had been uncaged. Lateral (E,G,I,K) and dorsal (I,J,K,L) views of embryos showing *foxd3* expression. Comparable patterns of *foxd3* expression were observed between wild-type (E,F) and CyHQ-*gad1b*-MO injected embryos raised in the dark (G,H). In contrast, the pattern of *foxd3* expression appeared expanded in CyHQ-*gad1b*-MO injected embryos raised in the light (I,J) and this expanded pattern was comparable to that observed in *gad1b* morphants (compare regions denoted by arrows and brackets).

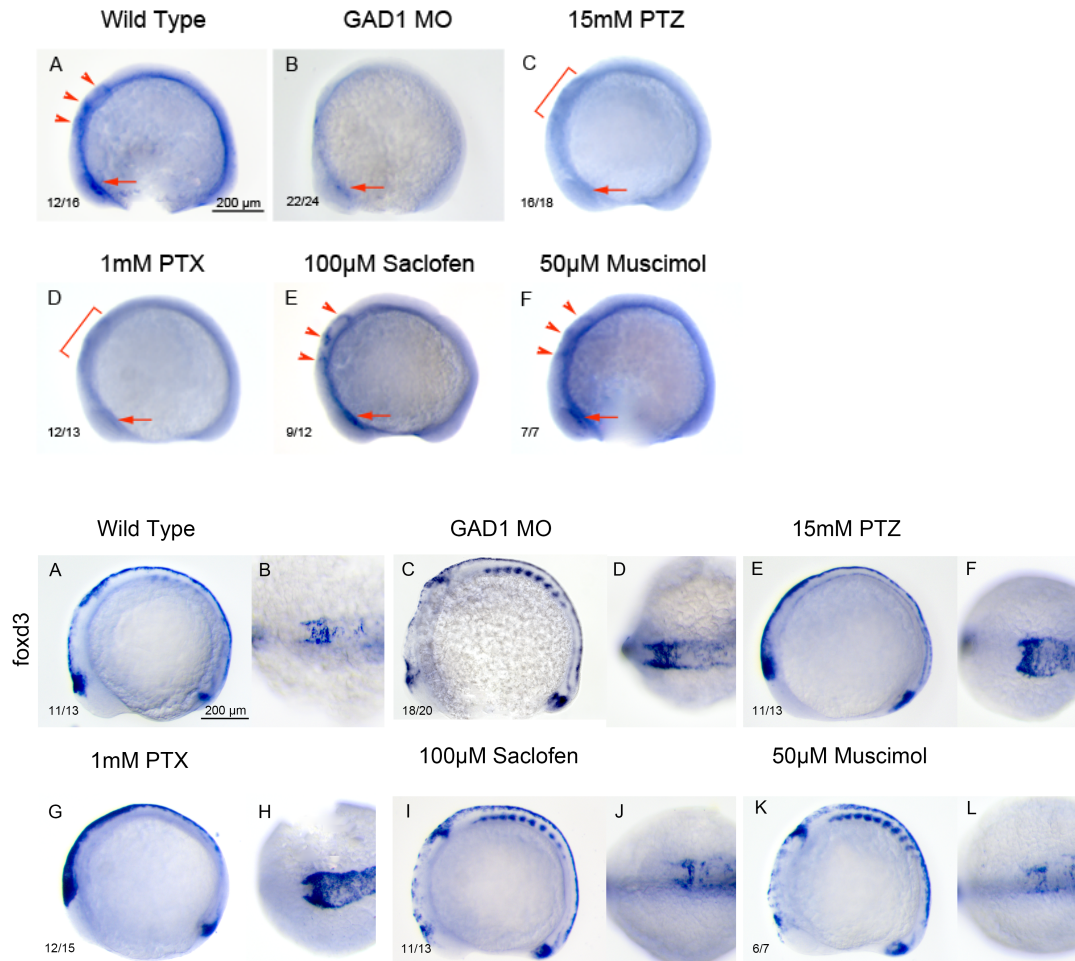


Figure S25. Treatment with GABA_A modulators phenocopy *gad1b* knockdown and exhibit reduced expression of *dlx2a* and altered expression of *foxd3*.

UPPER Panels: (A-F) Lateral view of ISH for *dlx2a* in wild-type, *gad1b* morphant (translation blocking), pentylentetrazol (PTZ) treated, picrotoxin (PTX) treated, saclofen treated and muscimol treated embryos at the 10-12 somite stage. (A-D) *dlx2a* expression is reduced in embryos treated with 15 mM PTZ or 1 mM PTX. PTZ and PTX are both GABA_A receptor antagonists. The reduction in expression is similar to that observed in *gad1b* morphant animals (arrow and bracket). Expression in the pharyngeal arches is almost absent, when compared to wildtype animals; (E) Animals treated with 100 µM saclofen, a GABA_B antagonists, exhibited *dlx2a* expression comparable to that of wild type animals (arrow and arrowheads); (F) Animals treated with 50 µM muscimol (a GABA_A agonist) exhibited a modest increase of *dlx2a* expression throughout the embryos, when compared to wild type animals.

LOWER Panels: Lateral (A,C,E,G,I,K) and dorsal (B,D,F,H,J,L) views of ISH for *foxd3* in wild-type, *gad1b* morphant (translation blocking), pentylentetrazol (PTZ) treated, picrotoxin (PTX) treated, saclofen treated and muscimol treated embryos at the 10-12 somite stage. The pattern of *foxd3* expression appeared expanded in embryos treated with 15 mM PTZ or 1 mM PTX

comparable to *gad1b* morphants. The pattern of *foxd3* expression in embryos treated with 100 μM saclofen or 50 μM muscimol was similar to that observed in wild-type embryos.

These findings support the idea that GABA signaling through the ionotropic GABA_A receptor plays a role in cranial neural crest cells.

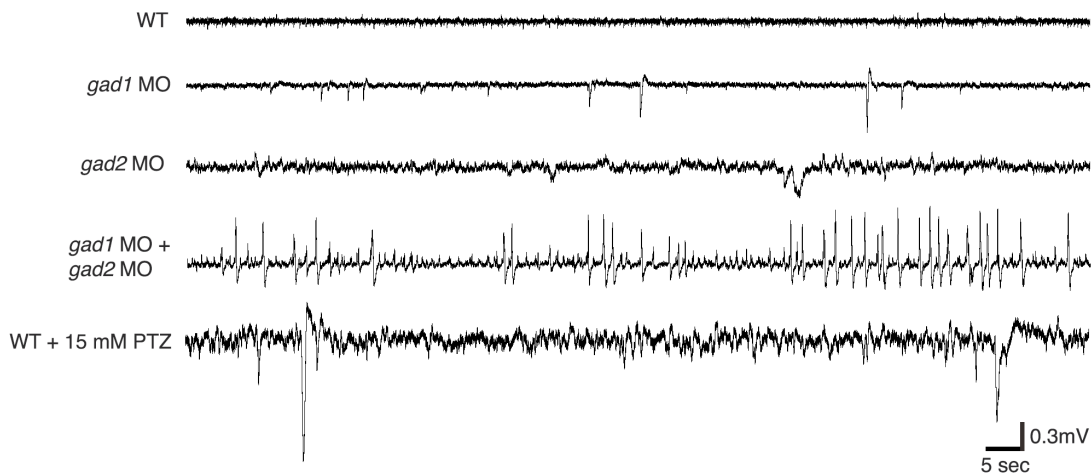


Figure S26. Knockdown of *gad1b* and *gad2* causes an increase in native neurological activity in 3 dpf zebrafish larvae.

(A) Native neurological activity within the optic tectum of 3 dpf wild-type animals. (B) Knockdown of *gad1b* causes an increase in the electrical activity observed in the optic tectum; note presence of events with amplitudes >0.3 mV. (C) Knockdown of *gad2* causes an increase in the electrical activity observed in the optic tectum; note increase in numbers of high frequency, low-amplitude events compared to WT. (D) *gad1b/gad2* double morphants exhibit a significant increase in neurological activity, when compared with either wild-type or single morphant animals. Large amplitude (>0.6 mV) events develop and occur in small clusters, separated by smaller (0.15 mV) events. (E) WT 3 dpf larva exposed to 15 mM PTZ for comparison.

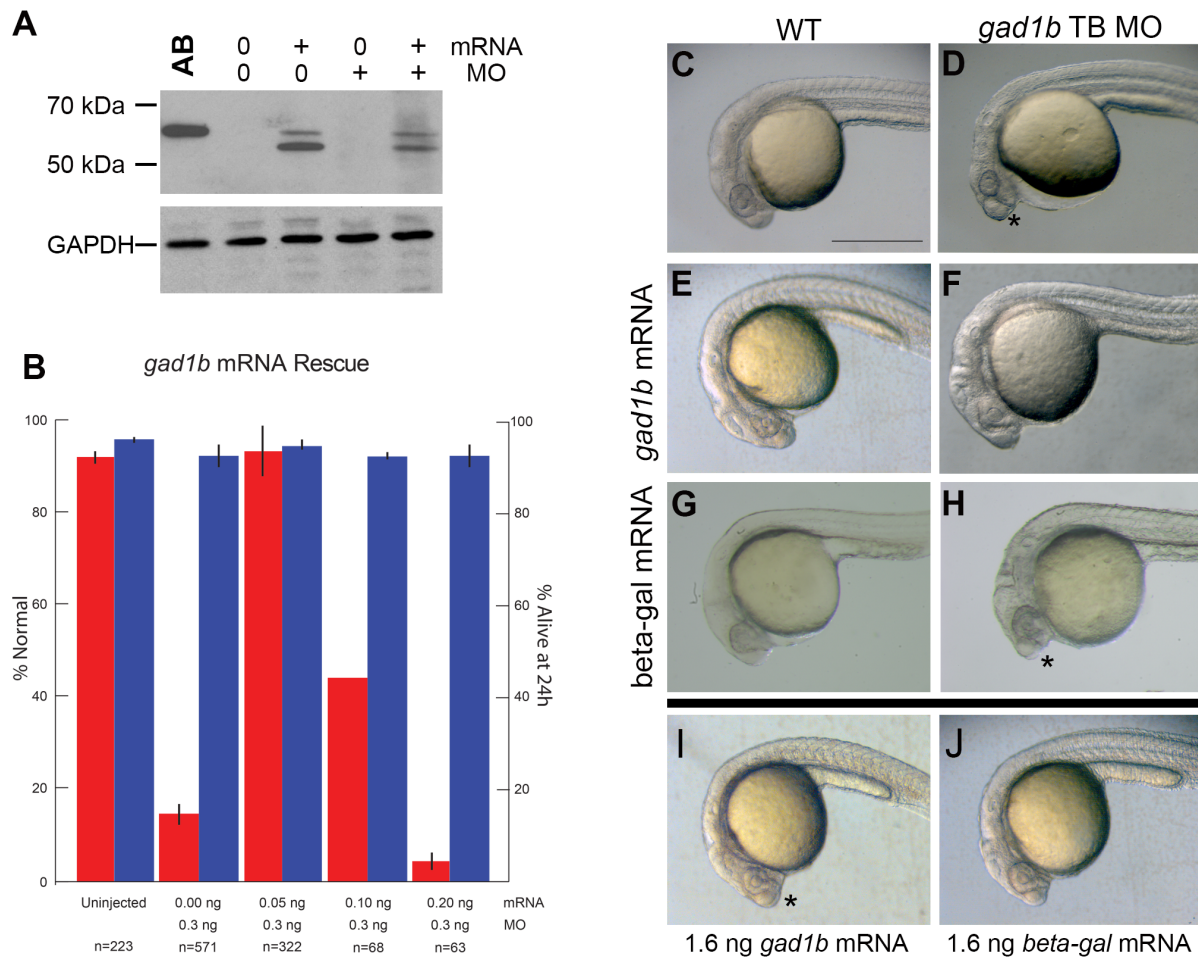


Figure S27. The *gad1b* synthetic mRNA is translated into Gad1b protein and can rescue morphant phenotype.

(A) Western blot analysis of Gad1 protein in pools of zebrafish embryos injected at the 1-4 cell stage with 0.1 ng capped *gad1b* mRNA, 0.3 ng *gad1b* translation blocking MO, or co-injected with 0.1 ng capped *gad1b* mRNA and 0.3 ng *gad1b* translation blocking MO. Protein extracts were prepared from 15 embryos at 1 dpf and quantitated using the bicinchoninic acid (BCA) assay (Pierce). Equal amounts of extract were loaded in each lane. Blots were probed using a mouse monoclonal to GAD₆₇ (K-87, cat # sc-58531, Santa Cruz Biotechnology Inc.). Protein extracts prepared from WT embryos and adult zebrafish brain (AB) served as positive controls. Injection of exogenous *gad1b* mRNA correlated with the detection of two Gad1 isoforms: one of the expected size of ~67 kDa and a second, smaller protein of ~61 kDa weight. The second isoform likely arose as a result of translation initiating from an internal in-frame ATG, most likely the ATG located in the region of the transcript corresponding with *gad1b* exon 3. See Figure S14. (B) Titration of *gad1b* synthetic mRNA for rescue experiments. Red bars represent the percent of injected animals (out of 100) that showed normal morphology; Blue bars represent the percent of injected animals alive at 24hpf. Error bars represent SEM. 0.05 ng of synthetic *gad1b* mRNA was sufficient to rescue early development of embryos injected with 0.3 ng *gad1b* translation blocking MO. (C-J). Representative images of embryos from rescue experiments. (C) Wild-type embryo for comparison. (E, G, I, J) Wild-type embryos injected with 0.05 ng synthetic

gad1b mRNA (E), 0.05 ng synthetic *beta-galactosidase* mRNA (G), 1.6 ng synthetic *gad1b* mRNA (I), or 1.6 ng synthetic *beta-galactosidase* mRNA (J). (D, F, H) Embryos injected with 0.3 ng *gad1b* translation blocking MO and (F) 0.05 ng synthetic *gad1b* mRNA or (H) 0.05 ng synthetic *beta-galactosidase* mRNA. Embryos co-injected with 0.05 ng synthetic *gad1b* mRNA and 0.3 ng *gad1b* translation blocking MO (F) exhibited more normal development than embryos injected with MO alone (D) or co-injected with synthetic *beta-galactosidase* mRNA (H), which exhibited smaller eyes and an altered distribution of the presumptive head mesenchyme (asterisks). Embryos injected with 0.05 ng synthetic *gad1b* mRNA (E), 0.05 ng synthetic *beta-galactosidase* mRNA (G), or 1.6 ng synthetic *beta-galactosidase* mRNA (J) exhibited normal morphological development. (I) Embryos injected with 1.6 ng synthetic *gad1b* mRNA exhibited altered head morphology similar to that observed in *gad1b* morphants. Scale bar A = 0.5 mm, applies to all panels.

Preparation of Synthetic *gad1b* mRNA

Construction of the gad1b clone for preparing synthetic gab1b mRNA.

The *gad1b* sequence was PCR-amplified using DreamTaq DNA Polymerase (Thermo Scientific) following manufacture's recommendations from cDNA prepared from adult brain using a forward primer, zf *gad1b* RNA rescue-F1-EcoRI:

5'-atta**GAATTCACCATG**GCAAGCAGCGCTCCATCTTCCTCGGCTGGTGATATG-3'
(52 nucleotides, 69.6 Tm)

and reverse primer, zf *gad1n* RNA rescue-R1-XhoI:

5'-attaCTCGAGTTACAGATCCTGACCGAGCC-3' (30 nucleotides, 62.1 Tm).

The primers were designed to amplify the native *gad1b* open reading frame while destroying the *gad1b* translation MO target site without codon alteration. Changes to the endogenous *gad1b* sequence around the translation initiation ATG (underlined) are denoted in bold in the forward primer. The sequence around the ATG meets the rules established for a Kozak sequence.^{24, 25} The primers included the following design features: 1) 4 nucleotides (ATTA), denoted in lowercase in the primer sequence, were added to the 5' end of each primer to ensure efficient cutting by restriction enzymes; and 2) EcoRI and XhoI sites were incorporated into the forward and reverse primers, respectively. The PCR amplicon was cloned into the EcoRI/XhoI sites of a modified pCS2+ vector^{26, 27} in which CMV promoter activity was destroyed by digestion with Sall and HindIII, subjected to end-repair using DNA Polymerase I large (Klenow) fragment (New England BioLabs), and self-ligated. The destruction of the CMV promoter permitted recovery of intact *gad1b* clones. Candidate clones were validated by sequencing.

In vitro transcription.

Capped *gad1b* mRNA lacking the *gad1b* translation blocking MO target sequence and beta-galactosidase mRNA (control, pCS2+nuclear localized lac Z) were synthesized *in vitro* using the mMessage mMachina Transcription Kit (Life Technologies, Grand Island, NY) following manufacturer's recommendations. Template plasmids were linearized by NotI digestion. RNA was synthesized using the using SP6 RNA polymerase. Reaction products were quantitated spectrophotometrically and assessed for size by denaturing gel electrophoresis.

Microinjection.

Capped mRNA was injected using pressure into one to four-cell stage embryos following standard protocols.²⁸⁻³¹ For rescue experiments, capped mRNA was co-injected with MOs. The same concentrations of *beta-galactosidase* mRNA were used in control experiments.

References

- (1) Ouyang, X., Shestopalov, I. A., Sinha, S., Zheng, G., Pitt, C. L. W., Li, W.-H., Olson, A. J., and Chen, J. K. (2009) Versatile Synthesis and Rational Design of Caged Morpholinos. *J. Am. Chem. Soc.* *131*, 13255-13269.
- (2) Davis, M. J., Kragor, C. H., Reddie, K. G., Wilson, H. C., Zhu, Y., and Dore, T. M. (2009) Substituent Effects on the Sensitivity of a Quinoline Photoremovable Protecting Group to One- and Two-Photon Excitation. *J. Org. Chem.* *74*, 1721-1729.
- (3) Den Dunnen, J. T., and Antonarakis, S. E. (2000) Mutation nomenclature extensions and suggestions to describe complex mutations: a discussion. *Hum. Mutat.* *15*, 7-12.
- (4) Schilling, T. F., and Kimmel, C. B. (1994) Segment and cell type lineage restrictions during pharyngeal arch development in the zebrafish embryo. *Development* *120*, 483-494.
- (5) Barrallo-Gimeno, A., Holzschuh, J., Driever, W., and Knapik, E. W. (2004) Neural crest survival and differentiation in zebrafish depends on mont blanc/tfap2a gene function. *Development* *131*, 1463-1477.
- (6) Lewis, J. L., Bonner, J., Modrell, M., Ragland, J. W., Moon, R. T., Dorsky, R. I., and Raible, D. W. (2004) Reiterated Wnt signaling during zebrafish neural crest development. *Development* *131*, 1299-1308.
- (7) Odenthal, J., and Nusslein-Volhard, C. (1998) Fork head domain genes in zebrafish. *Dev. Genes Evol.* *208*, 245-258.
- (8) Knight, R. D., Nair, S., Nelson, S. S., Afshar, A., Javidan, Y., Geisler, R., Rauch, G.-j., and Schilling, T. F. (2003) Lockjaw encodes a zebrafish tfap2a required for early neural crest development. *Development* *130*, 5755-5768.
- (9) O'Brien, E. K., d'Alencon, C., Bonde, G., Li, W., Schoenebeck, J., Allende, M. L., Gelb, B. D., Yelon, D., Eisen, J. S., and Cornell, R. A. (2004) Transcription factor Ap-2alpha is necessary for development of embryonic melanophores, autonomic neurons and pharyngeal skeleton in zebrafish. *Dev. Biol.* *265*, 246-261.
- (10) Powell, D. R., Hernandez-Lagunas, L., LaMonica, K., and Artinger, K. B. (2013) Prdm1a directly activates foxd3 and tfap2a during zebrafish neural crest specification. *Development* *140*, 3445-3455.
- (11) Kos, R., Reedy, M. V., Johnson, R. L., and Erickson, C. A. (2001) The winged-helix transcription factor FoxD3 is important for establishing the neural crest lineage and repressing melanogenesis in avian embryos. *Development* *128*, 1467-1479.
- (12) Lister, J. A., Cooper, C., Nguyen, K., Modrell, M., Grant, K., and Raible, D. W. (2006) Zebrafish Foxd3 is required for development of a subset of neural crest derivatives. *Dev. Biol.* *290*, 92-104.
- (13) Sasai, N., Mizuseki, K., and Sasai, Y. (2001) Requirement of FoxD3-class signaling for neural crest determination in *Xenopus*. *Development* *128*, 2525-2536.
- (14) Stewart, R. A., Arduini, B. L., Berghmans, S., George, R. E., Kanki, J. P., Henion, P. D., and Look, A. T. (2006) Zebrafish foxd3 is selectively required for neural crest specification, migration and survival. *Dev. Biol.* *292*, 174-188.
- (15) Kelsh, R. N., Dutton, K., Medlin, J., and Eisen, J. S. (2000) Expression of zebrafish fkd6 in neural crest-derived glia. *Mech. Dev.* *93*, 161-164.
- (16) Del Barrio, M. G., and Nieto, M. A. (2002) Overexpression of Snail family members highlights their ability to promote chick neural crest formation. *Development* *129*, 1583-1593.
- (17) Sefton, M., Sanchez, S., and Nieto, M. A. (1998) Conserved and divergent roles for members of the Snail family of transcription factors in the chick and mouse embryo. *Development* *125*, 3111-3121.

- (18) Wada, N., Javidan, Y., Nelson, S., Carney, T. J., Kelsh, R. N., and Schilling, T. F. (2005) Hedgehog signaling is required for cranial neural crest morphogenesis and chondrogenesis at the midline in the zebrafish skull. *Development* 132, 3977-3988.
- (19) Carney, T. J., Dutton, K. A., Greenhill, E., Delfino-Machin, M., Dufourcq, P., Blader, P., and Kelsh, R. N. (2006) A direct role for Sox10 in specification of neural crest-derived sensory neurons. *Development* 133, 4619-4630.
- (20) Chiang, E. F. L., Pai, C.-I., Wyatt, M., Yan, Y.-L., Postlethwait, J., and Chung, B.-c. (2001) Two Sox9 Genes on Duplicated Zebrafish Chromosomes: Expression of Similar Transcription Activators in Distinct Sites. *Dev. Biol.* 231, 149-163.
- (21) Blader, P., Straehle, U., and Ingham, P. W. (1996) Three Wnt genes expressed in a wide variety of tissues during development of the zebrafish, *Danio rerio*: developmental and evolutionary perspectives. *Dev. Genes Evol.* 206, 3-13.
- (22) Richman, J. M., and Lee, S.-H. (2003) About face: signals and genes controlling jaw patterning and identity in vertebrates. *BioEssays* 25, 554-568.
- (23) Knight, R. D., and Schilling, T. F. (2006) Cranial neural crest and development of the head skeleton. *Adv. Exp. Med. Biol.* 589, 120-133.
- (24) Kozak, M. (1992) Regulation of translation in eukaryotic systems. *Annu. Rev. Cell Biol.* 8, 197-225.
- (25) Kozak, M. (2001) A progress report on translational control in eukaryotes. *Sci. STKE* 2001, pe1.
- (26) Rupp, R. A. W., Snider, L., and Weintraub, H. (1994) *Xenopus* embryos regulate the nuclear localization of XMyoD. *Genes Dev.* 8, 1311-1323.
- (27) Turner, D. L., and Weintraub, H. (1994) Expression of achaete-scute homolog 3 in *Xenopus* embryos converts ectodermal cells to a neural fate. *Genes Dev.* 8, 1434-1447.
- (28) Sun, Y., Wloga, D., and Dougan, S. T. (2011) Embryological manipulations in zebrafish. *Methods Mol. Biol.* 770, 139-184.
- (29) Eisen, J. S., and Smith, J. C. (2008) Controlling morpholino experiments: don't stop making antisense. *Development* 135, 1735-1743.
- (30) Bill, B. R., Petzold, A. M., Clark, K. J., Schimmenti, L. A., and Ekker, S. C. (2009) A Primer for Morpholino Use in Zebrafish. *Zebrafish* 6, 69-77.
- (31) Stainier, D. Y. R., Raz, E., Lawson, N. D., Ekker, S. C., Burdine, R. D., Eisen, J. S., Ingham, P. W., Ingham, P. W., Schulte-Merker, S., Yelon, D., Weinstein, B. M., Mullins, M. C., Wilson, S. W., Ramakrishnan, L., Amacher, S. L., Neuhauss, S. C. F., Meng, A., Mochizuki, N., Panula, P., and Moens, C. B. (2017) Guidelines for morpholino use in zebrafish. *PLoS Genet.* 13, e1007000.